ALEPH 94-148
PHYSIC 94-129
19 September 1994

Limit on B_s° Oscillation Using a Jet-Charge Method

Owen Hayes, Hongbo Hu, Yi-Bin Pan, Jeffrey Turk, Sau Lan Wu, John Yamartino, Min Zheng

University of Wisconsin-Madison

Abstract

A preliminary lower limit is set on the B_s° meson oscillation parameter (Δm_s). All events with a high transverse momentum lepton and a reconstructible secondary vertex are used. The high transverse momentum leptons are produced mainly by b hadron decays, and the sign of the lepton indicates the particle/antiparticle final state in decays of neutral B mesons. The initial state is determined by a jet-charge technique using both sides of the event. Charged tracks consistent with a D_s meson vertex are combined into a reconstructed "charm" track, which then forms a vertex with the high transverse momentum lepton for the B_s decay point. The B_s meson momentum is reconstructed using an energy-flow technique. A maximum likelihood method is used to set a lower limit of $\Delta m_s > 4.0 \times 10^{-3}\ eV/c^2$ at the 95% confidence level. (Equivalently, $\Delta m_s > 6.0\ ps^{-1}$) Assuming a B_s° lifetime of $\tau_{B_s} = 1.5\,ps$ gives a limit of $x_s\ (\equiv \Delta m_s/\Gamma) > 9.0$. This analysis assumes that the fraction of b quarks that form B_s° mesons out of all b quarks produced in Z° decays is $12 \pm 4\%$.

1 Introduction

In the neutral K system, it is well-known that the physical states of definite masses are not K° and $\overline{K}^\circ$, but K_S and K_L, which are linear combinations of K° and $\overline{K}^\circ$. The same phenomenon occurs in the neutral B system: the physical states are not B_d°, $\overline{B}_d^\circ$, B_s° and $\overline{B}_s^\circ$, but B_{dS}, B_{dL}, B_{sS}, and B_{sL}. To a very good approximation, B_{dS} and B_{dL} are linear combinations of B_d° and $\overline{B}_d^\circ$, while B_{sS} and B_{sL} are linear combinations of B_s° and $\overline{B}_s^\circ$. The reason for the absence of mixing between the B_d° states and the B_s° states is that

$$m_{B_s} - m_{B_d} \sim 90\, MeV \tag{1}$$

and hence the diagonal elements of the Weisskopf-Wigner matrix are quite different in the B_d° and B_s° parts.

Unlike the neutral K system,where the lifetimes of K_S and K_L differ by a factor of 580, in the neutral B system the four lifetimes of B_{dS}, B_{dL}, B_{sS} and B_{sL} are all nearly the same. Consider either the B_d° system or the B_s° system. Let B° stand for either B_d° or B_s°, and $\overline{B}^\circ$ for either $\overline{B}_d^\circ$ or $\overline{B}_s^\circ$. If CP non-invariance, which is expected to be small, is neglected, then the probability that a meson created as B° (or $\overline{B}^\circ$) will be observed as a B° (or $\overline{B}^\circ$) is

$$P_u(t) = \frac{1}{2}e^{-\Gamma t}(1 + \cos \Delta m t), \tag{2}$$

where the subscript u denotes "unmixed", t is the proper time, Γ the width (inverse lifetime) of B_S or B_L, taken to be the the same, and Δm is the mass difference between B_S and B_L. Similarly, the probability that it will be observed as a $\overline{B}^\circ$ (or B°) is given by

$$P_m(t) = \frac{1}{2}e^{-\Gamma t}(1 - \cos \Delta m t), \tag{3}$$

where the subscript m stands for "mixed".

For the $B_d^\circ \overline{B}_d^\circ$ system, such time-dependent mixing has been observed by the ALEPH and OPAL Collaborations at LEP[1][2]. For the $B_s^\circ \overline{B}_s^\circ$ system, a lower limit for $\Delta m/\Gamma$ has been given by the ALEPH Collaboration[3]:

$$(\Delta m/\Gamma)_s > 2.0 \tag{4}$$

at the 95% confidence level. The limit in equation 4 was obtained using the event sample where a lepton with high transverse momentum (p_T) is found on each side of the event.

In this paper we investigate time-dependent $B_s^\circ \overline{B}_s^\circ$ mixing. Events are selected from $Z^\circ \rightarrow$hadrons, where there is at least one high p_T lepton. There is a significant increase in the event sample of this analysis over the dilepton analysis which requires two high p_T leptons. A jet-charge method is used to analyze the rest of the event. For example, in $Z^\circ \rightarrow b\bar{b}$ where $b \rightarrow c\ell^-\overline{\nu}$, the charge of the lepton has the same sign as that of the quark. Hence the particle/antiparticle state of the decay of the B_s° is determined by the sign of

$\|\cos\theta\| < 0.95$
approaches within 2.0 cm of the beam axis
within 10.0 cm in z at nearest approach to beam
≥ 4 TPC hits
$p < 45\ GeV/c$

Table 1: Track selection cuts used in hadronic event selection.

the lepton. The determination of the particle/antiparticle state of the B_s° at production is achieved by a rapidity weighted jet-charge technique using information from both sides of the event. In the determination of Δm_s, the method of maximum likelihood is used to study the fractions of mixed and unmixed events as a function of the decay distances (proper times) of the B_s° mesons which undergo semileptonic decays.

2 Event Selection

This analysis is based on approximately 1.7 million hadronic Z° decays collected in the ALEPH experiment during the 1991–1993 data runs.

A detailed description of the ALEPH detector is available elsewhere[4]. The vertex detector (VDET) consists of two layers of double-sided silicon strip microstrip detectors. The inner layer is at an average radius of 6.3 cm from the beam axis, and covers 85% of the solid angle. The outer layer is at 10.8 cm, and covers 69% of the solid angle. The point resolution at normal incidence is 12 μm in both the z and $r\phi$ projections. Charged tracks are measured in an inner tracking chamber (ITC) of outer radius 26 cm, followed by a time projection chamber (TPC) from 40 to 171 cm in radius. The momentum resolution for charged tracks combining VDET, ITC and TPC information in the 1.5 Tesla magnetic field is $\delta p/p = 0.0006p\,(GeV/c)^{-1}$ for high momentum tracks. The TPC also provides up to 330 measurements of specific ionization ($\mathrm{d}E/\mathrm{d}x$) with 4.6% resolution. The electromagnetic calorimeter (ECAL), situated within the superconducting solenoidal magnet, is used with the TPC to identify electrons. The ECAL energy resolution is $\sigma(E)/E = 0.18/\sqrt{E}$ (E in GeV). The hadronic calorimeter (HCAL) and the muon chambers surrounding it are used to identify muons. The total thickness of the calorimeter system is more than 8 interaction lengths.

Events are selected which have at least five tracks satisfying the criteria of Table 1. The momentum sum of these tracks must exceed 10% of the LEP energy. In each event the charged and neutral particles (determined by an energy-flow algorithmal:eflow) are separated into jets using the scaled-invariant-mass technique[5] with the y_c parameter set at 0.02. Events are then searched for leptons. If an event has one or more leptons satisfying the criteria of Table 2, the highest momentum lepton is selected. The highest

Electrons:	Muons:
$p > 2.0\ GeV/c$	$p > 3.0\ GeV/c$
$\lvert\cos\theta\rvert < 0.92$	$\lvert\cos\theta\rvert < 0.94$
≥ 5 TPC hits	≥ 4 TPC hits
closest approach to beam axis $<$ 5 mm, and within 10 cm of interaction point in z at closest approach	closest approach to beam axis $<$ 5 mm, and within 10 cm of interaction point in z at closest approach
ECAL energy profile consistent with electron ($R_T > -1.6$)	$\geq$ 40% of expected HCAL planes register hits (number expected must be ≥ 10)
good ECAL longitudinal profile ($-1.8 < R_L < 3.0$)	excess hit multiplicity < 1.5 in the last 10 HCAL planes
if dE/dX info is available (for ≥ 50 wires), then: dE/dX yield not more than 2.5σ lower than the expected yield for electrons (no upper limit)	≥ 5 HCAL hits in the last 10 planes
no γ–conversion partner with opposite charge within 1.0 cm in the $x - y$ plane where the tracks are parallel, within 1.0 cm in z at that point, and with invariant mass $<$ $0.020\ GeV/c^2$	≥ 1 HCAL hit in the last 3 planes
	≥ 1 muon chamber hit

Table 2: Summary of the lepton selection criteria for muons and electrons.

component	number	fraction (%)
$B_s^\circ \to l$	1679	8.3
$B_d^\circ \to l$	5666	28.1
other $b \to l$	7988	39.6
$b \to c \to l$	1975	9.8
other background	2852	14.2
total	20160	100.0

Table 3: Monte Carlo composition of high p_T leptons sources.

momentum lepton in the hemisphere opposite from the first is also selected if one is found. The leptons are associated with their nearest jets. These are referred to as the same side and opposite side jets (with respect to each lepton). If only one lepton is found, the jet forming the highest invariant mass with the jet closest to the lepton is selected as the opposite side jet. The event is required to have the thrust axis away from the beam axis ($|\cos(\theta_{thrust})| < 0.85$).

The transverse momentum (p_T) of the lepton from its associated jet is calculated with the lepton momentum first subtracted from that of the jet. The lepton is required to have p_T greater than 1.0 GeV/c. These leptons are mainly produced by b hadrons, as they have sufficient mass to produce the large transverse momentum. The b hadron source fraction of the leptons is further enhanced by looking for evidence of a displaced b hadron in the opposite hemisphere. The QVSRCH package[6] used in this analysis for separating a displaced heavy meson decay vertex from the interaction point features a variable (BTAG) which uses evidence of displaced vertices to discriminate against light quark background contamination. (QVSRCH and the BTAG variable it returns are described in the next section.) A cut of 4.0 in the BTAG variable for the jet in the opposite hemisphere is used. A Monte Carlo simulation is used to estimate the different contributions to the selected event sample. The composition for the sources of high p_T leptons (after final selection) is shown in Table 3.

3 Decay Length Reconstruction

The interaction point and decay vertex position must be reconstructed to determine the decay length of the b hadron. The decay length reconstruction here is the same as was used in the dilepton analysis[3]. The QVSRCH [6] package is used to separate charged tracks consistent with primary vertex origin from those that appear to be the products of a displaced heavy meson decay vertex. Tracking information from all charged tracks in

75 successive hadronic events is used in a common fit to estimate the beam position and size in the $r\phi$ projection.

The beam position can be measured to $30\,\mu$m in x and $10\,\mu$m in y. The typical RMS of the spot size is $150\,\mu$m in x and $10\,\mu$m in y.

The primary vertex position is reconstructed as follows: A coarse z coordinate is found using tracks which pass within 3 mm of the beam axis. The tracks which pass within the cylinder of ± 3 mm of this z point, and 3 mm from the beam axis, are extrapolated into the plane defined by the measured y position of the beam. The y position of the beam is known to $10\,\mu$m, and is used as the y coordinate of the primary vertex. Grid points are spaced $20\,\mu$m apart in both x and z on this plane, and serve as candidate primary vertex positions. The χ^2 for each candidate vertex position is calculated using the impact points and errors of all tracks within three standard deviations of the candidate vertex point. The beam position and size in the x coordinate are also used in the χ^2 calculation. A paraboloid is fit to the χ^2 values of the grid points to interpolate the best primary vertex position. The curvature of the paraboloid gives the vertex error. The resolution in b hadron events is typically $90\,\mu$m along the flight direction.

Charged tracks which are in the same hemisphere as the high p_T lepton (excluding the lepton itself) are assigned to either the interaction point or a single reconstructed displaced decay vertex. A grid point search is performed for the secondary vertex position to find the displaced vertex point – track assignment combination that has the greatest difference in χ^2 when compared to the case where all tracks are assumed to come from the interaction point. (Some charged tracks may remain unassigned if they are not compatible with either of these vertices.) The magnitude of this difference in χ^2 gives evidence of a displaced heavy meson decay vertex and is used in the opposite hemisphere to enhance the b hadron purity of the event sample. This is the BTAG variable mentioned in the Event Selection section. Tracks within 1.7σ of the displaced vertex point are combined to form a reconstructed charm track. If only one track passes this condition, it serves as the charm track. At least one of the tracks in the charm vertex is required to have a vertex detector hit. The charm track is then intersected with the lepton to form a candidate B_s° decay vertex. The lepton is required to have at least one vertex detector hit. The χ^2/NDF for the reconstructed B vertex is required to be less than 10. The decay length (l_{dcy}) of the b hadron is projected along the jet direction. The Monte Carlo decay length resolution is shown in Fig 1. A parameterization of the resolution to three offset gaussians is used in the treatment of Section 6. The parameters are listed in Table 4.

4 Boost Reconstruction

The relativistic boost of the B meson must be estimated in order to calculate its proper lifetime. The method used in this analysis has been described in the ALEPH dilepton mixing analysis[3]. The meson momentum is the sum of the lepton momentum,

Table 4: Decay Length Resolution (fit to three gaussians)

Area (%)	Sigma (μm)	Offset (μm)
33.6	218	58
43.1	612	66
23.3	2.3 mm	-416

Table 5: Boost Resolution (fit to two gaussians)

Area (%)	Sigma (%)	Offset (%)
50.4	9	-2.4
49.6	26.8	-7.9

the momentum of the charged tracks assigned to the D vertex, the estimated neutrino momentum, and a fraction of the measured neutral jet momentum. The neutrino energy is estimated as the difference between the beam energy and the amount of visible energy[7] in the hemisphere containing the lepton. The B meson is assigned its typical contribution of 67% of the visible neutral momentum of the jet. This fraction is taken from the Monte Carlo.

An boost term (g_{true}) is defined as $m_{true}c/p_{true}$ (in terms of the true mass (m_{true}) of the appropriate b hadron), so that the proper time in terms of the true decay distance (l_{true}) is simply:

$$t_{true} = g_{true}\, l_{true}. \tag{5}$$

The reconstructed boost is parameterized in terms of the reconstructed momentum as:

$$g = \frac{220}{p_{rec} + 8.4} \left(\frac{ps}{cm}\right), \tag{6}$$

where p_{rec} is in GeV/c. The resolution in g is plotted in Fig 2. The boost resolution is parameterized as two gaussians whose parameters are listed in Table 5.

The reconstructed proper time is defined as:

$$t_{rec} = g\, l_{dcy}. \tag{7}$$

We require $|t_{rec}| < 14$ ps.

5 Determination of $B^\circ/\overline{B}^\circ$ States at Production and Decay

To determine whether the B° meson of semileptonic decay has undergone mixing or not, it is important to determine the flavour (b or $\bar{b}$) of this B° meson at production time ($t = 0$). A jet charge technique has been used for this purpose by OPAL[2], using momentum weighted charge. We present here a new jet charge method using rapidity weighted charge. The jet charge is defined as

$$Q_{jet} = \frac{\sum_{i=1}^{n} y_i q_i}{\sum_{i=1}^{n} y_i}, \tag{8}$$

where y_i is the rapidity defined as:

$$y_i = \ell n \frac{E_i + P_{i||}}{E_i - P_{i||}}, \tag{9}$$

and where q_i is the charge of track i and E_i and $P_{i||}$ are the energy and momentum component along the jet axis of track i. The jet charges of both sides of the event are used. The purpose is to determine the b flavour (B° or $\overline{B}^\circ$) at production time ($t = 0$) of the jet containing the high-p_T lepton. The flavour of the jet at decay time is determined by the charge of the high-p_T lepton.

The following example illustrates how this rapidity weighted jet-charge method works better than the traditional momentum weighted jet-charge method. The momentum weighted jet-charge is defined as

$$Q'_{jet} = \frac{\sum_{i=1}^{n} P_{i||}^{\kappa} q_i}{\sum_{i=1}^{n} P_{i||}^{\kappa}}, \tag{10}$$

where $\kappa = 1$. Consider the case where the lepton side (same side) contains a $\bar{b}$ quark at production and the opposite side contains a b quark at production. Fig 3(a) shows Q'_{jet} on the opposite side (Q'^{o}_{jet}) which centers at a negative value, as expected from a b quark (negative charge), and Fig 3(b) shows Q'_{jet} on the same side as the lepton (Q'^{s}_{jet}) which centers at a positive value as expected from a $\bar{b}$ quark (positive charge). Fig 4(a) shows Q'_{jet} on the same side as the lepton (Q'^{s}_{jet}) for events where a $\bar{b}$ quark at production has undergone mixing and produces a negatively charged lepton. The Q'^{s}_{jet} centers at a negative value, in contrast to the expectation of a $\bar{b}$ quark at production. The unmixed distribution is shown in Fig 4(b). This undesirable result is caused by the fact that the charge of the energetic lepton carries a strong weight. For unmixed events, Q'^{s}_{jet} centers correctly at the positive value corresponding to the expectation of a $\bar{b}$ quark at production.

On the other hand, using the rapidity weighted events, the incorrect sign of Q'^{s}_{jet} for mixed events shown in Fig 4(a) is not present. Fig 5(a) and Fig 5(b) show that Q^{o}_{jet} (b jet)

and Q^s_{jet} ($\overline{b}$ jet) center correctly at negative and positive values respectively. Likewise Q^s_{jet} ($\overline{b}$ jet) for mixed events and Q^s_{jet} ($\overline{b}$ jet) for unmixed events center correctly at positive values as shown by Fig 6(a) and Fig 6(b).

A powerful variable to tag mixed or unmixed events is

$$Q = Q^s_{jet} - Q^\circ_{jet}. \tag{11}$$

Fig 7(a) and Fig 7(b) show $Q' = Q'^s_{jet} - Q'^\circ_{jet}$ for mixed and unmixed events respectively, using the momentum weighted jet-charge method. For the mixed events, $Q' = Q'^s_{jet} - Q'^\circ_{jet}$ center at a negative value in contrast to an expectation of positive value($q_{\overline{b}} - q_b$ =positive). For unmixed events, $Q' = Q'^s_{jet} - Q'^\circ_{jet}$ center correctly at a positive value. However, using the rapidity weighted method, Fig 8(a) and Fig 8(b) show that $Q = Q^s_{jet} - Q^\circ_{jet}$ centers correctly at positive values for both mixed and unmixed events. Fig 9 shows that Monte Carlo and data distributions in $Q = Q^s_{jet} - Q^\circ_{jet}$ agree well.

To tag events as mixed and unmixed events, we define, for negative charged lepton events:

$$Q = (Q^s_{jet} - Q^o_{jet}) > 0.2 \qquad mixed \tag{12}$$

$$Q = (Q^s_{jet} - Q^o_{jet}) < -0.2 \qquad unmixed \tag{13}$$

and for positive charged lepton events:

$$Q = (Q^s_{jet} - Q^o_{jet}) < -0.2 \qquad mixed \tag{14}$$

$$Q = (Q^s_{jet} - Q^o_{jet}) > 0.2 \qquad unmixed \tag{15}$$

With this selection, 69% of truly mixed events have their mixed/unmixed state correctly determined, and 84% of unmixed events are correctly determined. The efficiency for the cut at 0.2 is approximately 50%. Note that these "tag rates" are calculated for events where the lepton comes directly from a semileptonic b decay. These tag rates are degraded in subsequent sections by including the effects of leptons from other sources. The major source of leptons with the wrong sign is the semileptonic decays of the charm daughters of b hadron decays. The total number of selected decays in the tagged mixed and unmixed samples are 5502 and 17176, respectively.

6 Method of Maximum Likelihood

The purpose of this section is to discuss in some detail the method of maximum likelihood. As seen from equations (2) and (3), the most important variable for the analysis of time-dependent $B^\circ_s - \overline{B}^\circ_s$ oscillation is the proper time t for the decay of the B°_s or $\overline{B}^\circ_s$. Therefore, in this section we shall first discuss the treatment of this proper time.

The first important observation is that t is not measured directly. Rather, it is obtained through two *independent* measurements:

$$\frac{t}{\tau_b} = t_1 t_2 \ , \tag{16}$$

where the boost t_1 and the dimensionless decay distance t_2 are given by

$$t_1 = g_{true} \ \ and \ \ t_2 = \frac{l_{true}}{\tau_b c} \ , \tag{17}$$

and τ_b is the lifetime of the various b hadrons, taken to be equal. The masses of the various b hadrons are also assumed equal to a common mass (m_b) of 5.3 GeV/c^2 (between the B_s° and B_d° masses).

In equation (16), t_1 and t_2 are the true values of the boost and the dimensionless decay distance. Let s_1 and s_2 be the corresponding measured values. Then the conditional probability distributions $P_1(s_1|t_1)$ and $P_2(s_2|t_2)$ are independent. Here, for example, $P_1(s_1|t_1)$ is the probability distribution of the measured value s_1 of the boost for a given value of the actual boost t_1. To a good approximation[3] this $P_1(s_1|t_1)$ is given by the sum of the two Gaussians of Table 5, while the $P_2(s_2|t_2)$ is given by the sum of the three Gaussians of Table 4.

Let $D_o(p_b)$ be the momentum distribution of the B meson, then it is given to a good approximation by the Peterson form. A change of variable from p_b to t_1 then gives the joint distribution in t_1 and t_2 as

$$D(t_1, t_2) = \begin{cases} \frac{1}{\tau_b} \frac{m_b}{t_1} D_o(\frac{m_b}{t_1}) e^{-t_1 t_2} & \text{for } t_1 > \frac{m_b}{E_{beam}} \text{ and } t_2 > 0 \\ 0 & \text{otherwise.} \end{cases} \tag{18}$$

With this $D(t_1, t_2)$, the joint distribution in t_1, t_2, s_1 and s_2 is then

$$P(t_1, t_2, s_1, s_2) = D(t_1, t_2) P_1(s_1|t_1) P_2(s_2|t_2). \tag{19}$$

With the relation given in equation (19), the method of maximum likelihood can be developed in a straightforward manner. The following parameters play important roles:

f_{B_d} is the fraction of B_d° mesons in the sample;

f_{B_s} is the fraction of B_s° mesons in the sample;

f_{udsc} is the fraction of events in the sample which have the non-b hadron lifetime τ_{udsc};

τ_{udsc} is the lifetime of the component of uds and c events that do not have lifetime τ_b;

$x_d = |\Delta m_d|\tau_b$ is the mixing parameter for B_d°;

$x_s = |\Delta m_s|\tau_b$ is the mixing parameter for B_s°;

and there are two tag rates:

A_u is the fraction of unmixed events correctly tagged as unmixed; and

A_m is the fraction of mixed events correctly tagged as mixed.

With the method of jet charge described in Section 5, these two tag rates, A_u and A_m, turn out to be different in value.

In terms of the above parameters, we define

$$\alpha_m(t) = \frac{1}{2} f_{B_s}(1 - \cos x_s t) + \frac{1}{2} f_{B_d}(1 - \cos x_d t). \tag{20}$$

The probability distribution $P(t_1, t_2, s_1, s_2)$ of equation (19) is used to get the desired mixed and unmixed distributions by

$$\beta_m(s_1, s_2) = \int_o^\infty dt_1 \int_o^\infty dt_2 \; \alpha_m(t_1 t_2) P(t_1, t_2, s_1, s_2), \tag{21}$$

and

$$\beta_u(s_1, s_2) = \int_o^\infty dt_1 \int_o^\infty dt_2 \; [1 - \alpha_m(t_1 t_2)] P(t_1, t_2, s_1, s_2). \tag{22}$$

We now consider non-b hadron ($udsc$) background events. These events are treated as unmixed b hadrons, except for the shorter lifetime. The reconstructed proper time distribution measured in the MC 2 sample (see Section 8) is fitted with two exponentials. It turns out that one component ($\sim 30\%$) has a lifetime of 1.5 ps, close to the b hadron lifetime, while the other component ($\sim 70\%$) has a much smaller lifetime (0.16 ps). The first component is conveniently combined with the contributions from b hadrons that do not oscillate. While the total fraction of non-b hadron events is $\sim 14\%$, f_{udsc} is the $\sim 10\%$ ($14\% \times 70\%$) of events which have the smaller lifetime of 0.16 ps. To include this type of background, equation (22) is modified as follows:

$$\beta_u(s_1, s_2) = \int_o^\infty dt_1 \int_o^\infty dt_2 \; [1 - f_{udsc} - \alpha_m(t_1 t_2)] P(t_1, t_2, s_1, s_2) \; + \int_o^\infty dt_1 \int_o^\infty dt_2 \; f_{udsc} P(t_1, t_2, s_1, s_2; \tau_{udsc}), \tag{23}$$

where $P(t_1, t_2, s_1, s_2; \tau_{udsc})$ is the same as in equation (19), except that now the $D(t_1, t_2)$ defined in equation (18) is calculated using τ_{udsc} instead of τ_b.

Finally, if $N_m(N_u)$ is the number of events where the method of jet charge as described in Section 3 gives the result that the event is mixed (unmixed), then the likelihood function is given by

$$L = \prod_{i=1}^{N_m} [A_m \beta_m(s_{1i}, s_{2i}) + (1 - A_u)\beta_u(s_{1i}, s_{2i})] \prod_{j=1}^{N_u} [(1 - A_m)\beta_m(s_{1j}, s_{2j}) + A_u \beta_u(s_{1j}, s_{2j})]. \tag{24}$$

Table 6: Fit values (and input values for Monte Carlo) from a 2-dimensional fit for the B_d° mixing parameter (Δm_d), and unmixed tag rate (A_u).

		Δm_d	A_u
DATA		0.544 ± 0.043	0.792 ± 0.004
MC 2	Inputs: $\Delta m_d = 0.467$ $A_u = 0.790$	0.484 ± 0.049	0.789 ± 0.004

7 B_d° oscillation as a check

The B_d° oscillation parameter (Δm_d) is determined as a check on the analysis. Fixing $\tau_b = 1.5$ ps, $f_{B_s} = 0.12$, $f_{B_d} = 0.373$, $\Delta m_s = 30ps^{-1}$, $A_m = 0.60$, a two-dimensional grid of likelihood functions in Δm_d and A_u gives $\Delta m_d = 0.544 \pm 0.043$ and $A_u = 0.792 \pm 0.004$.

Table 6 gives the values for Δm_d and A_u both for the data and Monte Carlo. For the Monte Carlo sample the fitted values for Δm_d and A_u agree well with the input values.

Fig 10 shows the like-sign fraction for (a) the Monte Carlo reconstructed events and (b) the data.

8 The Study of Δm_s with Monte Carlo Data Samples

Two samples of Monte Carlo simulated hadronic events are used to study the sensitivity of Δm_s, one with 1.62 million events with $\tau_B = 1.3ps$ (MC 1) and one with 1.34 million events with $\tau_B = 1.5ps$ (MC 2). Figs 11(a) to (d) and Figs 12(a) to (d) show the $\Delta \log L$ distribution as a function of Δm_s for different Δm_s input values for MC 1 and MC 2. Here, $\Delta \log L = (\log L)_{\Delta m_s} - (\log L)_{\Delta m_s = 14}$. ($\log L$ beyond $\Delta m_s = 14$ stays constant). From these two Monte Carlo samples, clear signals can be seen up to about $\Delta m_s = 5ps^{-1}$.

9 The likelihood curve for the data

Fig 13 shows the $\Delta \log L$ curve for the data as a function of Δm_s. It is calculated using the central values of the parameters listed in Table 7. The Δm_d used is the result of the fit done in section 7. The parameter f_{bc} is the fraction of selected events containing a b hadron where the lepton is produced at the "cascade" charm decay vertex. f_{bc} is taken from MC 2 and assigned an approximate 10% error. f_{B_d} is estimated in the dilepton analysis[3] as 0.37 ± 0.03. f_{B_s} is assumed to be $12 \pm 4\%$. (This assumption is now under study.)

Table 7: Inputs to the fit and the toy Monte Carlo.

Parameter	
Δm_d	0.544 ± 0.05
f_{bc}	0.093 ± 0.01
f_{B_d}	0.37 ± 0.03
f_{B_s}	0.12 ± 0.04

Table 8: Correct tag rates (A_u) for various unmixed b hadrons.

Hadron	A_u (%)
B_d°	76.3 ± 0.6
B_s°	77.6 ± 1.2
other	80.9 ± 0.4
average	79.0 ± 0.3

The decay length resolution for the data is parameterized as 10% worse than what is measured in the Monte Carlo[3]. Also shown in Fig 13 are the curves given by the $\Delta \log L$ for each input Δm_s (measured at the input) for MC 1 and MC 2. The average of these two curves is also plotted.

In the fit for the unmixed tag rate A_u (see Section 7), all unmixed b hadrons are assumed to have the same tag rate. This is nearly true in the Monte Carlo, as can be seen in Table 8. To check the sensitivity of the fit to the tag rate used, A_u for B_s° mesons was changed by $\pm 4\%$ from the average, and A_u for other events was changed so that the average A_u remained unchanged. Only small differences appear in the $\log L$ curve near 5 or 6 ps^{-1}.

10 Check of the b hadron lifetime

Fixing A_u and Δm_d as determined in Section 7, the maximum likelihood method of Section 6 gives $\tau_b = 1.34 \pm 0.02\ ps$ for the data, and $\tau_b = 1.36 \pm 0.04\ ps$ for one fourth of the MC 2 Monte Carlo sample with input $\tau_b = 1.5\ ps$. The low reconstructed lifetime is caused by a decay length dependent efficiency. This effect can be treated by weighting events at longer decay lengths appropriately to account for this loss in efficiency. When the efficiency is correctly accounted for, the fit for the lifetime in the data yields $\tau_b = 1.52 \pm 0.02\ ps$, and $\tau_b = 1.49 \pm 0.04\ ps$ for the same fourth of the MC 2 Monte Carlo sample (input lifetime of $\tau_b = 1.5\ ps$). The loss in efficiency is only significant for events

at large decay length ($l_{dcy} > 1$ cm). Since these events are less than one percent of the total sample, the efficiency correction has a no visible effect on the data $\Delta \log L$ curve. Note that this check of the b hadron lifetime was performed using a BTAG selection on both sides of the event. Although the selection on the same side is no longer used, the result is not expected to change.

11 Setting the Limit for Δm_s

A toy Monte Carlo technique is used to set the limit for Δm_s. The toy Monte Carlo data samples are generated based on key observed distributions in MC 2. A true momentum and decay length is generated for each $b \rightarrow l$ event. The true momentum is generated according to the true momentum distribution of b hadrons in $b \rightarrow l$ decays (measured in MC 2 after the final event selection), and the true decay length is calculated using the true momentum and a true proper time generated using an exponential decay-time distribution (with $\tau_b = 1.5$ ps). The decay length and momentum resolutions vary as functions of true decay length and true momentum respectively, and the values are smeared accordingly.

The decay length and momentum generation is done similarly for cascade decays ($b \rightarrow c \rightarrow l$), using the corresponding momentum and decay length resolution distributions. In addition, the measured extra decay time due to the charm lifetime is added to the generated proper time, producing a longer decay length.

The jet charge of the event is then simulated based on the measured jet charge distributions of each species of b hadron (mixed and unmixed) in MC 2. For B_d° and B_s° mesons, the mixed/unmixed state of the meson is chosen according to the probabilities of equations 2 and 3. The observed lepton sign is then chosen according to whether the lepton comes from a direct semileptonic b hadron decay, a subsequent cascade decay, or from some other source. The generated rates of these sources are based on their measured abundances in MC 2. The jet charge value and lepton sign tag the mixed/unmixed state of the decay.

The charm and *uds* contributions are simulated in a slightly different way. The reconstructed decay length and momentum distributions, also from MC 2 (after final selection), are used to generate events. The fraction of these events which are tagged mixed and unmixed events is made to match what is measured in MC 2.

In generating a "toy" Monte Carlo data sample, the relative contributions of each of the above types of decays are set according to the composition of MC 2 after the final event selection (see Table 3). To account for systematic uncertainties, the toy Monte Carlo further includes gaussian smearing of the parameters shown in Table 7 by the listed errors. The likelihood differences ($\Delta \log L$) are then the $\log L$ calculated at the input value of Δm_s, minus the $\log L$ calculated for maximal mixing ($\Delta m_s = 30$) for the different input values. This is carried out for about 100 samples at each input Δm_s (2.0, 4.0, 5.0, 6.0

and 7.0), each with sample size equal to that of the data. Figures 14(a) and (b) show the $\Delta \log L$ distribution for input $\Delta m_s = 5\, ps^{-1}$ and $\Delta m_s = 6\, ps^{-1}$. Fig 15 shows the same MC 1 and MC 2 likelihood curves (and their average) as in Fig 13. The superimposed average $\Delta \log L$ values for various inputs of Δm_s in the toy Monte Carlo indicate good agreement with the full Monte Carlo.

The 95% confidence limit curve is determined in the following way: The distribution of $\Delta \log L$ (for an input Δm_s) is fitted to a single gaussian with the 95% confidence point as one of the parameters. Fig 16(a) shows the points below which lie (by counting rather than fitting) exactly 95% of the $\Delta \log L$ values of the generated samples. Plotted in Fig 16(b) are the 95% confidence limit points obtained by fitting. These 95% confidence points are then fitted (as a function of Δm_s) to a second order polynomial, and the resulting curve is taken as the starting point for the 95% confidence limit curve.

However, the second order polynomial should be modified so that the curve asymptotically approaches zero from above. In addition, there is an error on the curve due to the limited number of toy monte carlo samples. To account for these and further possible systematic errors, the 95% confidence limit curve was raised by 1.4 $\log L$ units. This amount was chosen in part to avoid the shoulder just above 6 ps^{-1}. This procedure was performed to keep the limit estimate conservative.

The (raised) 95% confidence limit curve of Fig 16(b) intersects the data $\Delta \log L$ curve at 6.0 ps^{-1}. This is taken as the preliminary estimate of the lower limit for Δm_s.

12 Conclusions

A preliminary 95% confidence limit of $\Delta m_s > 6.0\ ps^{-1}$ is set using a maximum likelihood technique. This corresponds to $4.0 \times 10^{-3}\ eV/c^2$. Using $\tau_{B_s} = 1.5\, ps$ would give a limit of $x_s\ (\equiv \Delta m_s/\Gamma) > 9.0$. In this analysis the fraction (f_{B_s}) of b quarks that form B_s° mesons (with respect to all b quarks produced in Z° decays) is assumed to be $12 \pm 4\%$. This assumption is now under study. Other work in progress involves finalizing the limit curve by increased toy Monte Carlo statistics.

References

[1] D. Buskulic *et al.* (ALEPH Collab.), Phys.Lett.B**313** (1993) 498.

[2] R. Akers *et al.* (OPAL Collab.), Phys.Lett.B**327** (1994) 411.

[3] D. Buskulic *et al.* (ALEPH Collab.), Phys. Lett. B**322** (1994) 441.

[4] D. Decamp *et al.* (ALEPH Collab.), Nucl. Inst. Methods A**294** (1990) 121.

[5] S. Bethke *et al.* (JADE Collab.), Phys. Lett. B**213** (1988) 235.

[6] T. Mattison , ALEPH Note 92-173 (December 1992).

[7] D. Buskulic *et al.* (ALEPH Collab.), Phys. Lett. B**246** (1990) 306.

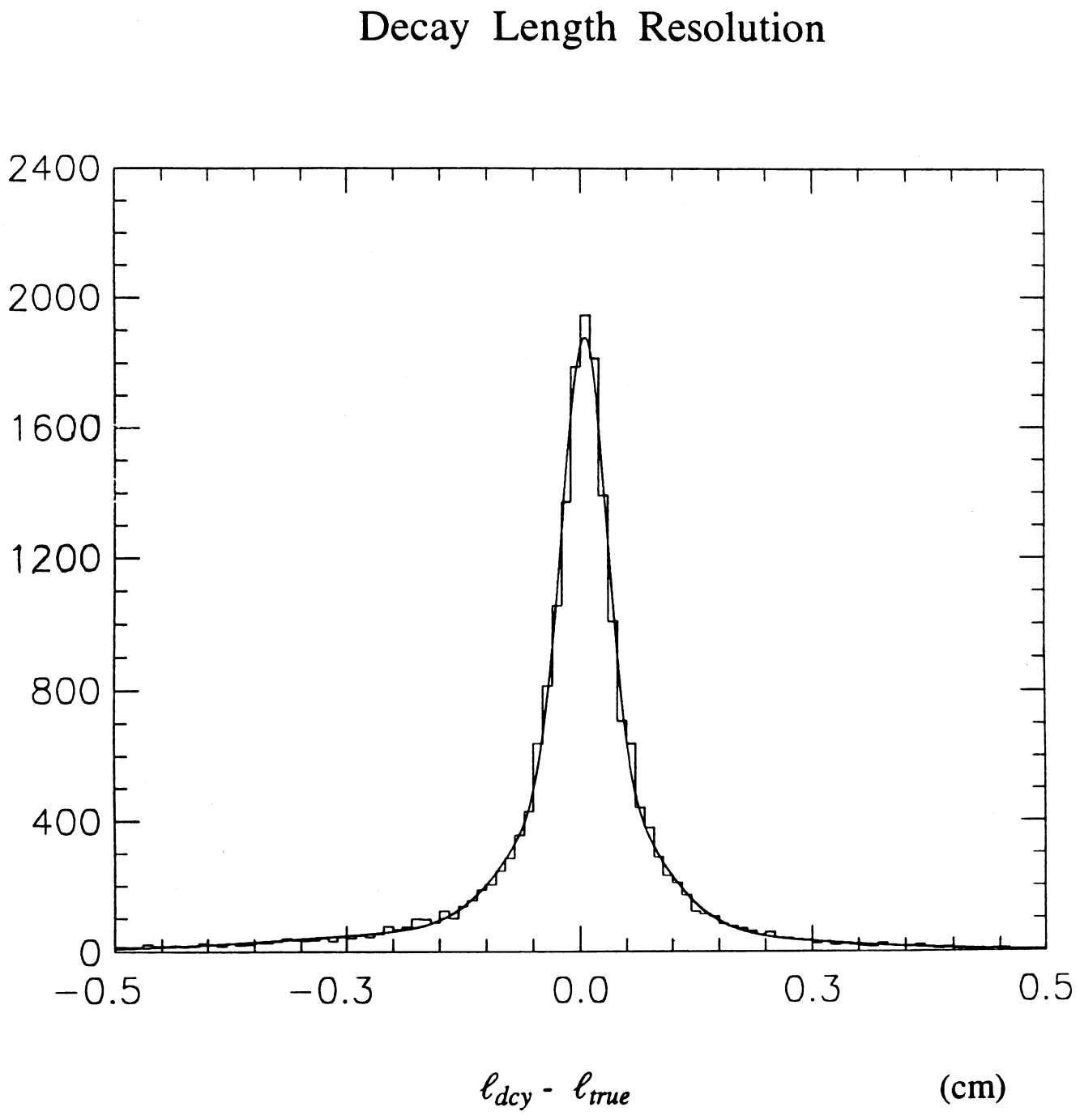

Figure 1. Decay length resolution.

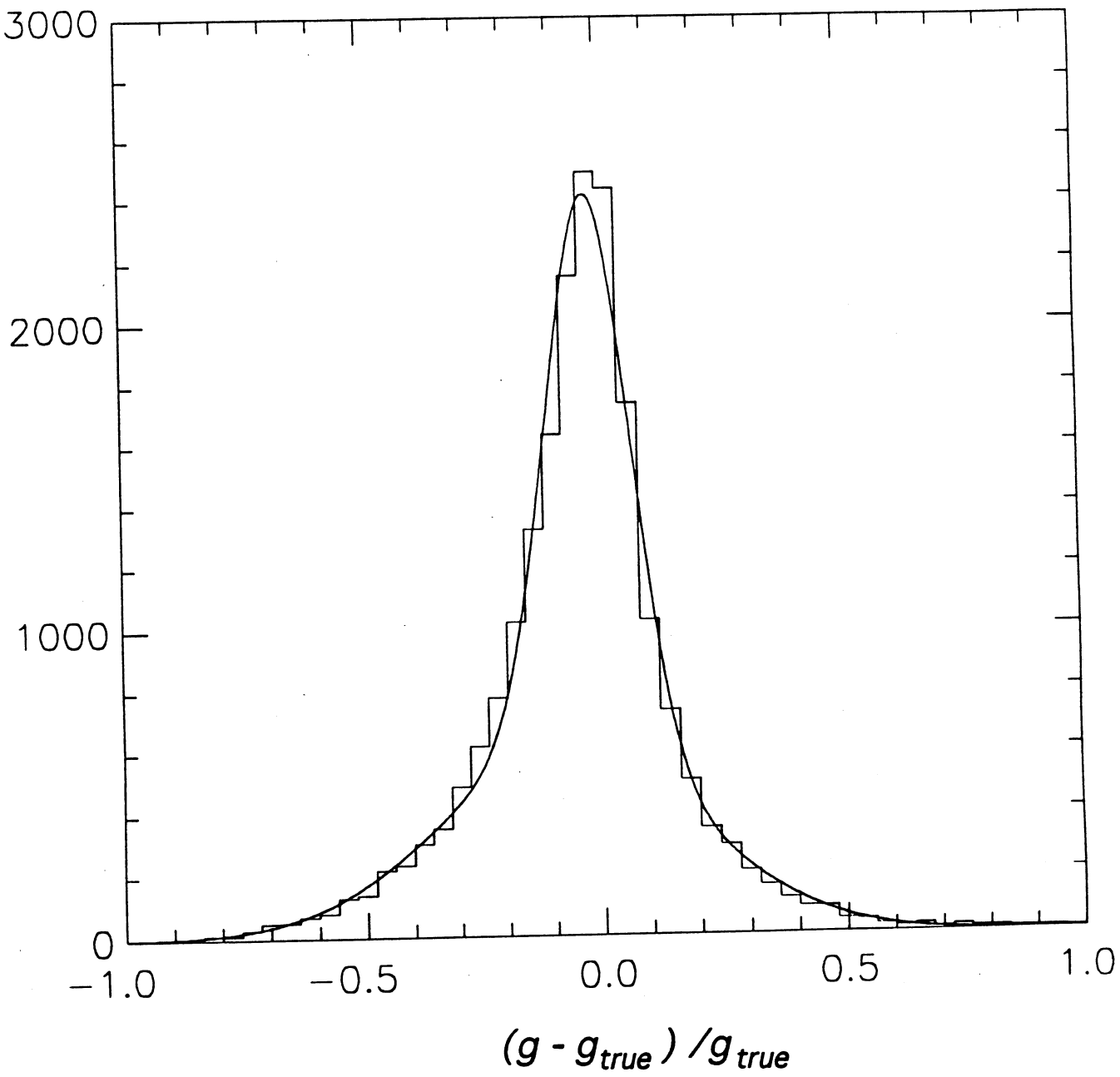

Figure 2. "Boost" resolution.

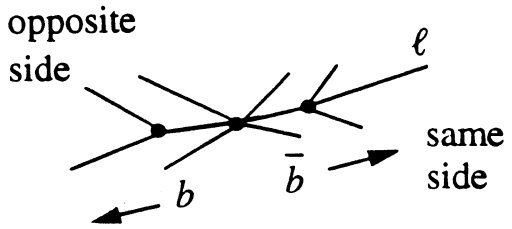

$$Q'_{jet} = \frac{\Sigma\, p_{i//}\, q_i}{\Sigma\, p_{i//}}$$

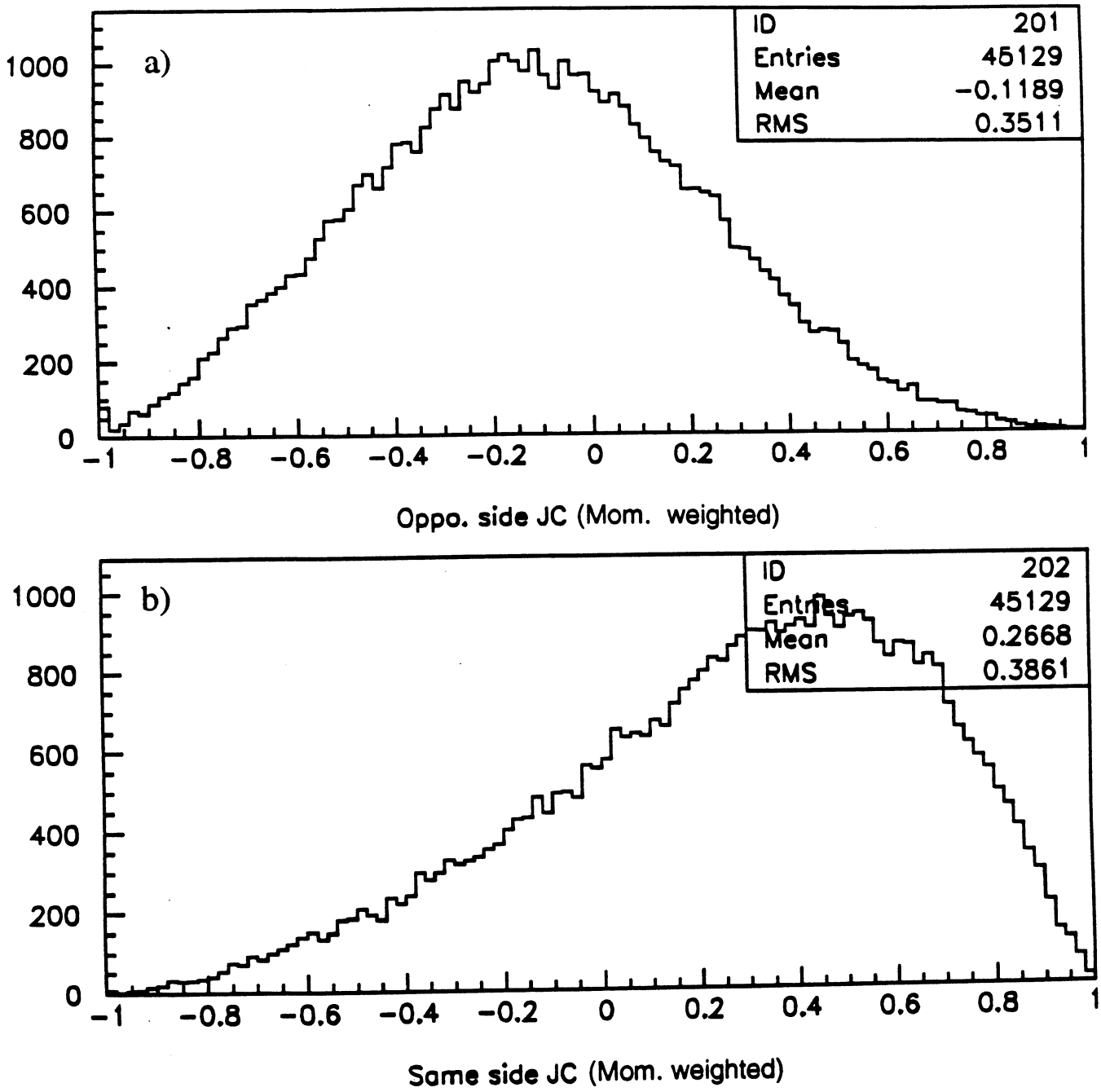

Figure 3. Momentum weighted jet charge distributions for a) the opposite side, and b) the same side (for initial state $\bar{b}$ quarks).

Same Side Momentum Weighted Jet Charge

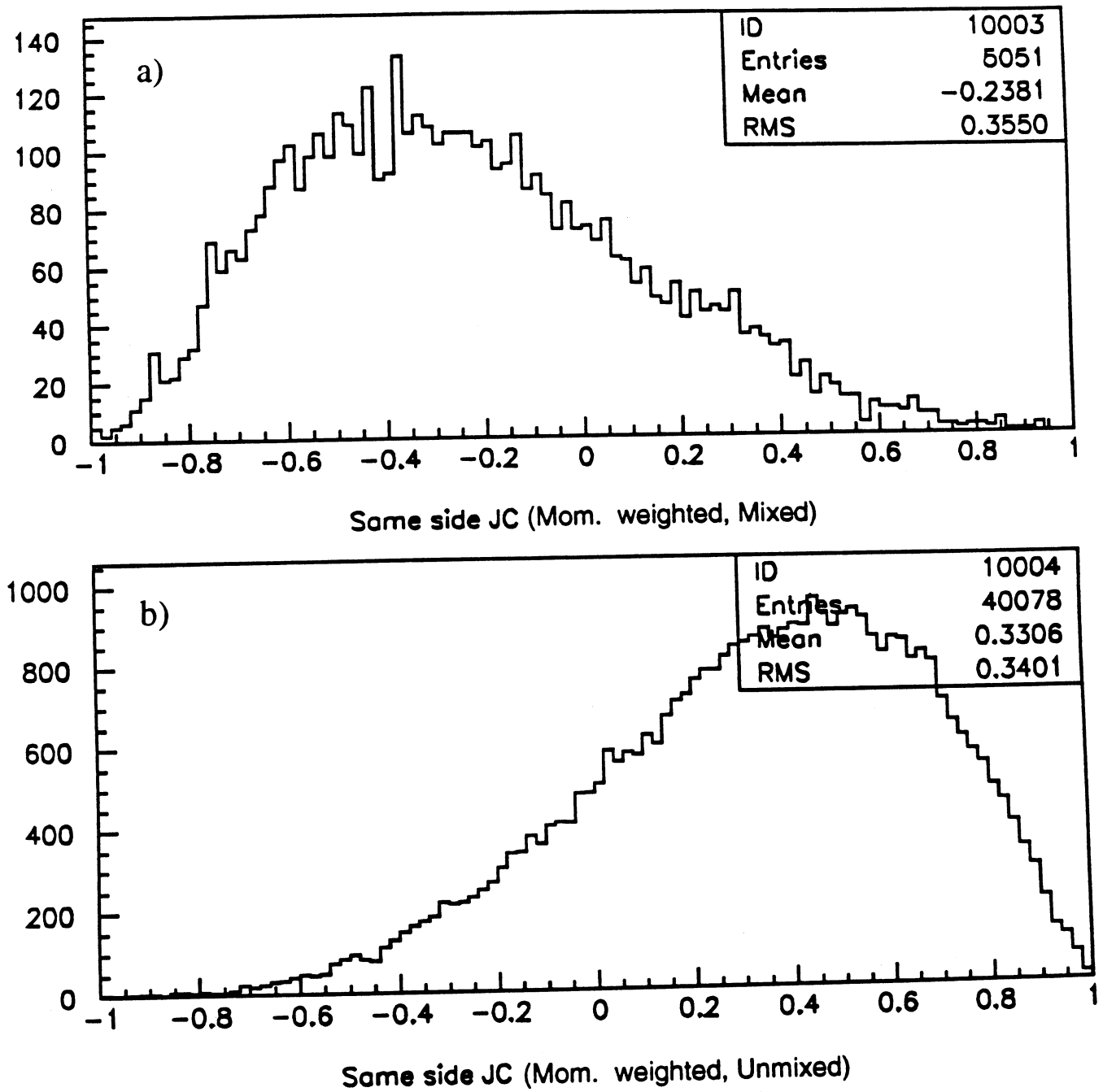

Figure 4. Momentum weighted jet charge distributions on the same side as an initial state $\bar{b}$ quark for a) mixed B^o mesons, and b) unmixed b hadrons.

Rapidity Weighted

$$y_i = \ln \frac{E_i + P_{i//}}{E_i - P_{i//}} \qquad Q_{jet} = \frac{\Sigma\, y_i\, q_i}{\Sigma\, y_i}$$

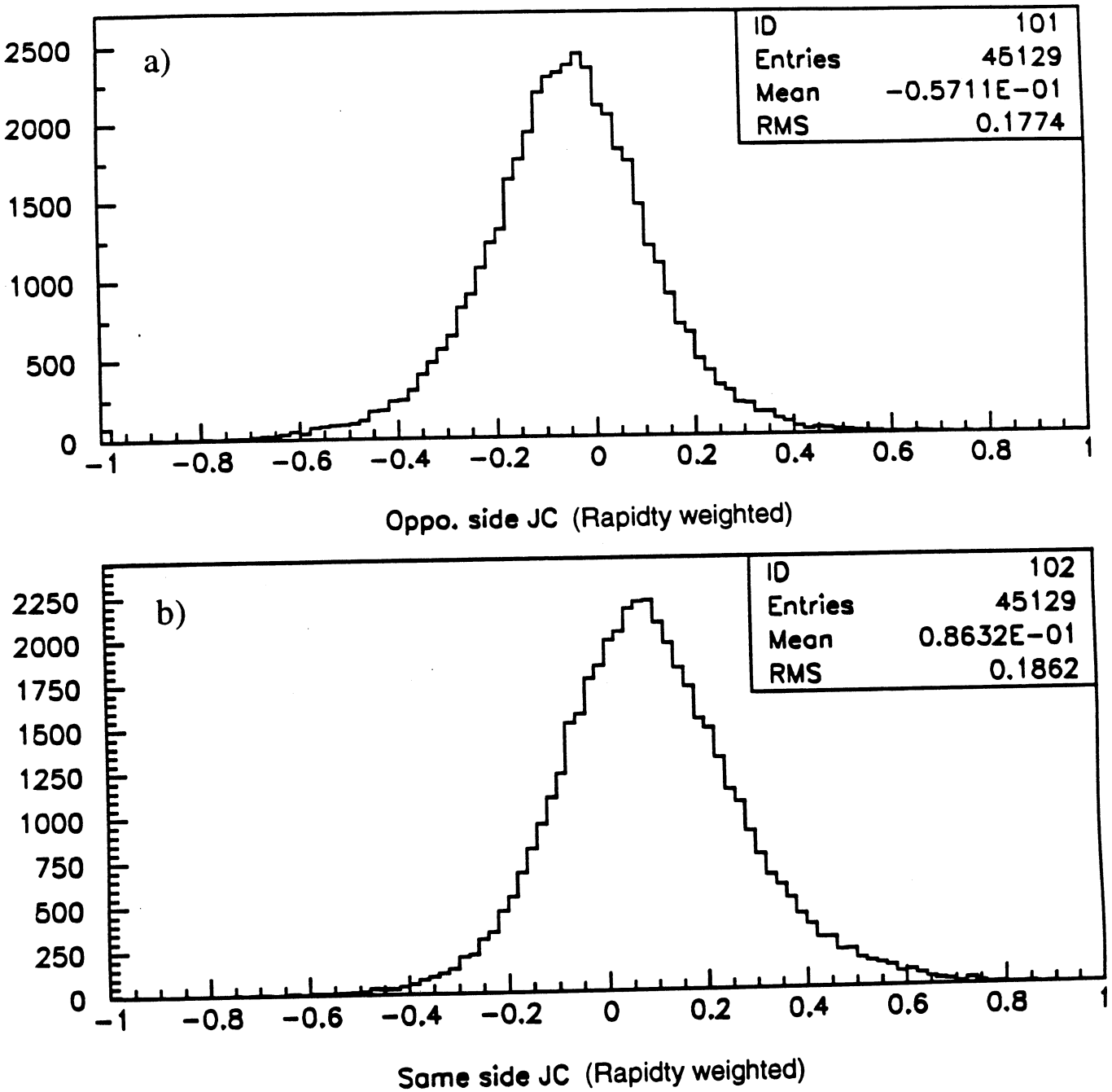

Figure 5. Rapidity weighted jet charge distributions for a) the opposite side, and b) the same side (for initial state $\bar{b}$ quarks).

Same Side Rapidity Weighted

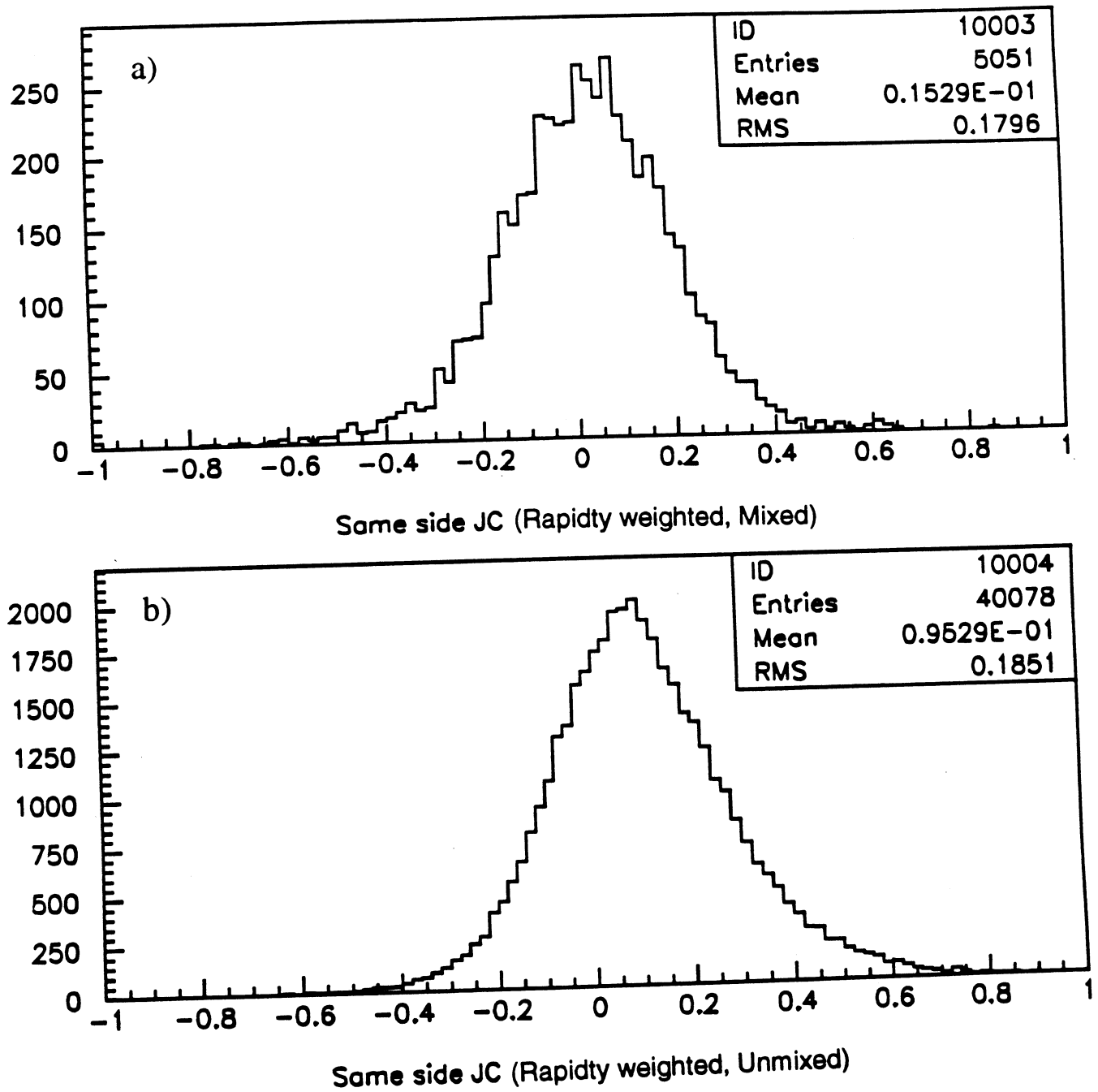

Figure 6. Rapidity weighted jet charge distributions on the same side as an initial state $\bar{b}$ quark for a) mixed B^o mesons, and b) unmixed b hadrons.

$$Q^{'s}_{jet} - Q^{'o}_{jet}$$

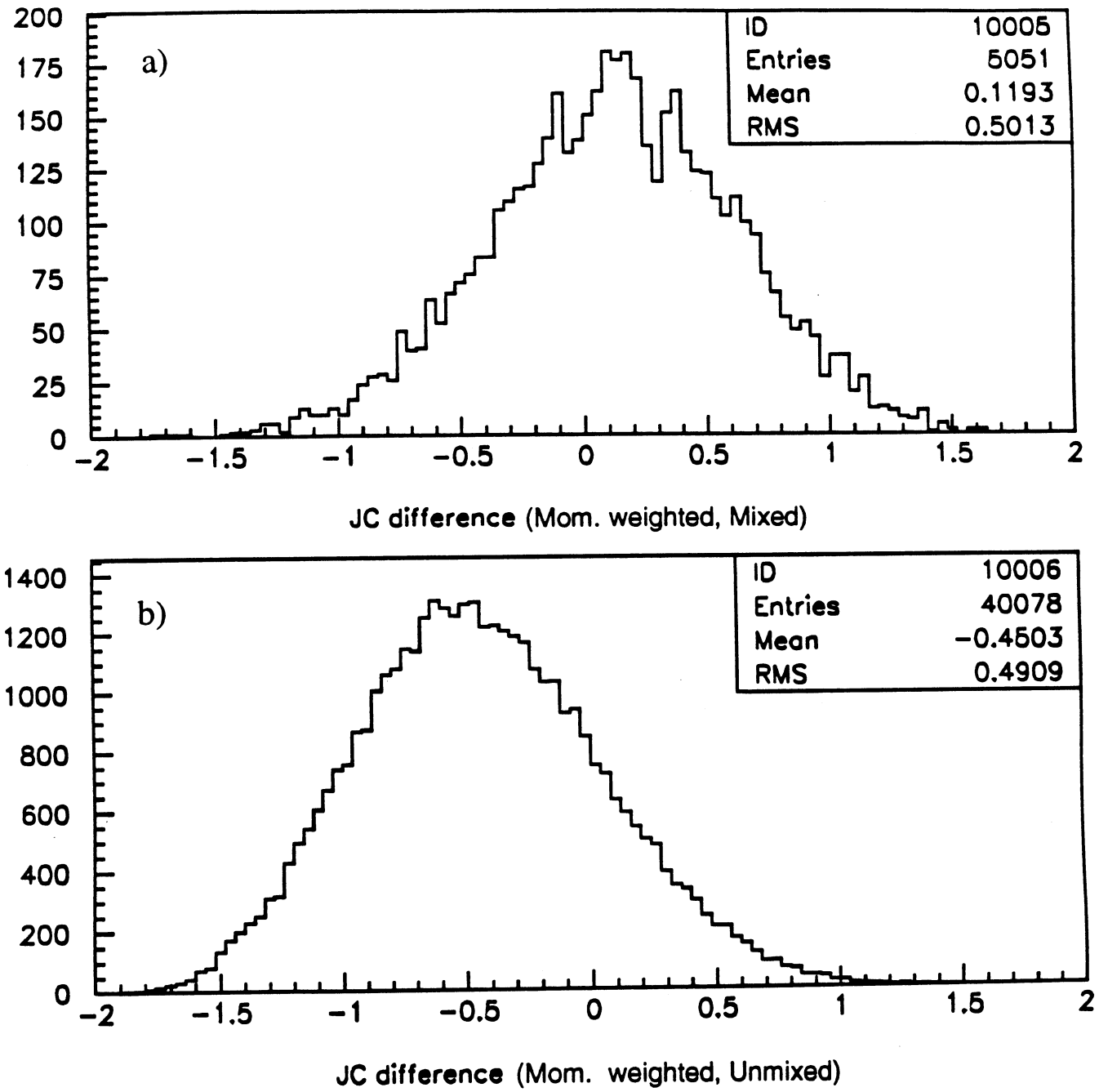

Figure 7. Same side minus opposite side momentum weighted iet charge distributions for an initial state $\bar{b}$ quark for a) mixed B^o mesons, and b) unmixed b hadrons.

$$Q^s_{jet} - Q^o_{jet}$$

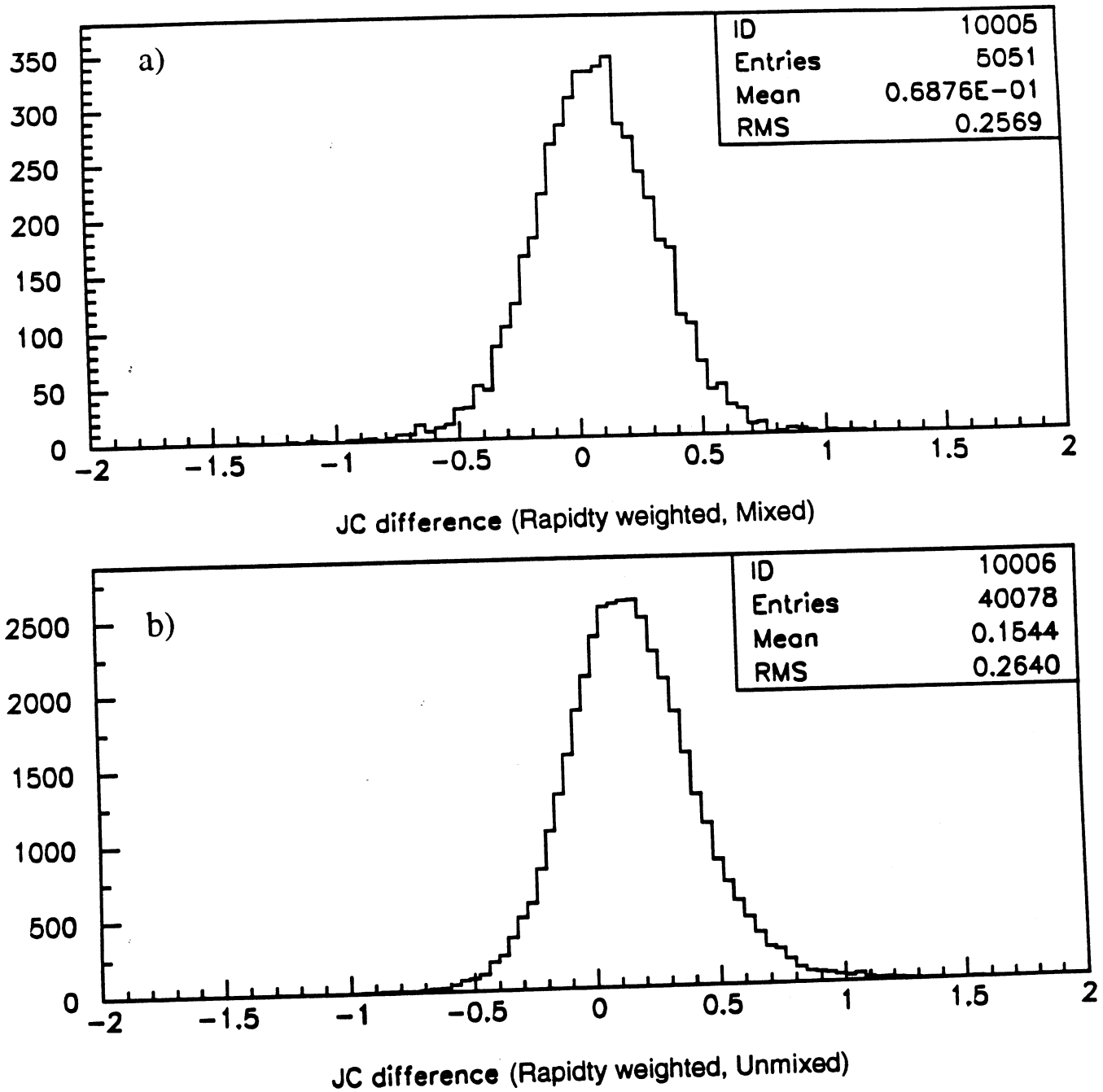

Figure 8. Same side minus opposite side rapidity weighted jet charge distributions for an initial state $\bar{b}$ quark for a) mixed B^o mesons, and b) unmixed b hadrons.

$$Q^s_{jet} - Q^o_{jet}$$

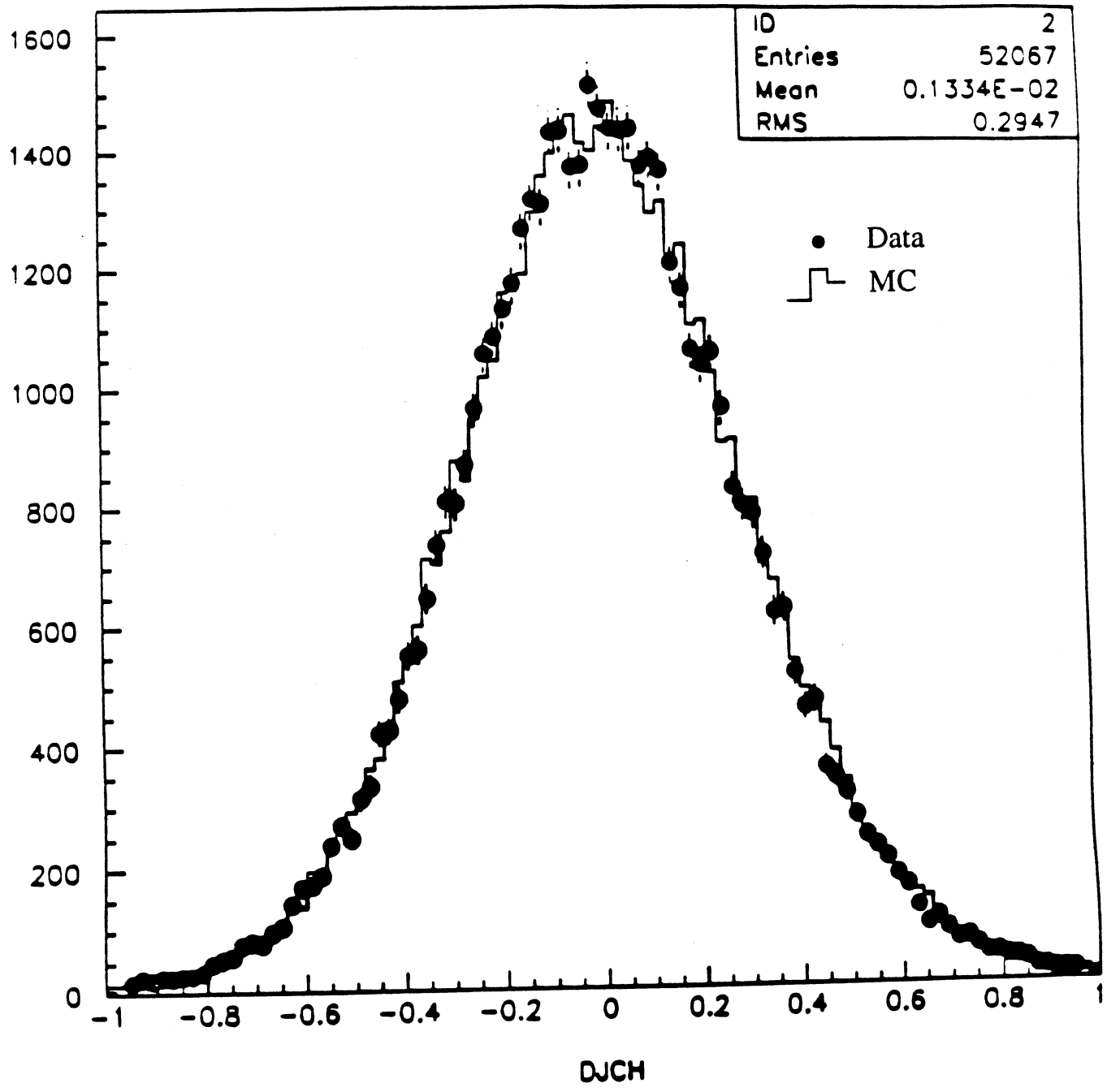

Figure 9. Same side minus opposite side rapidity weighted jet charge distributions for the data and Monte Carlo.

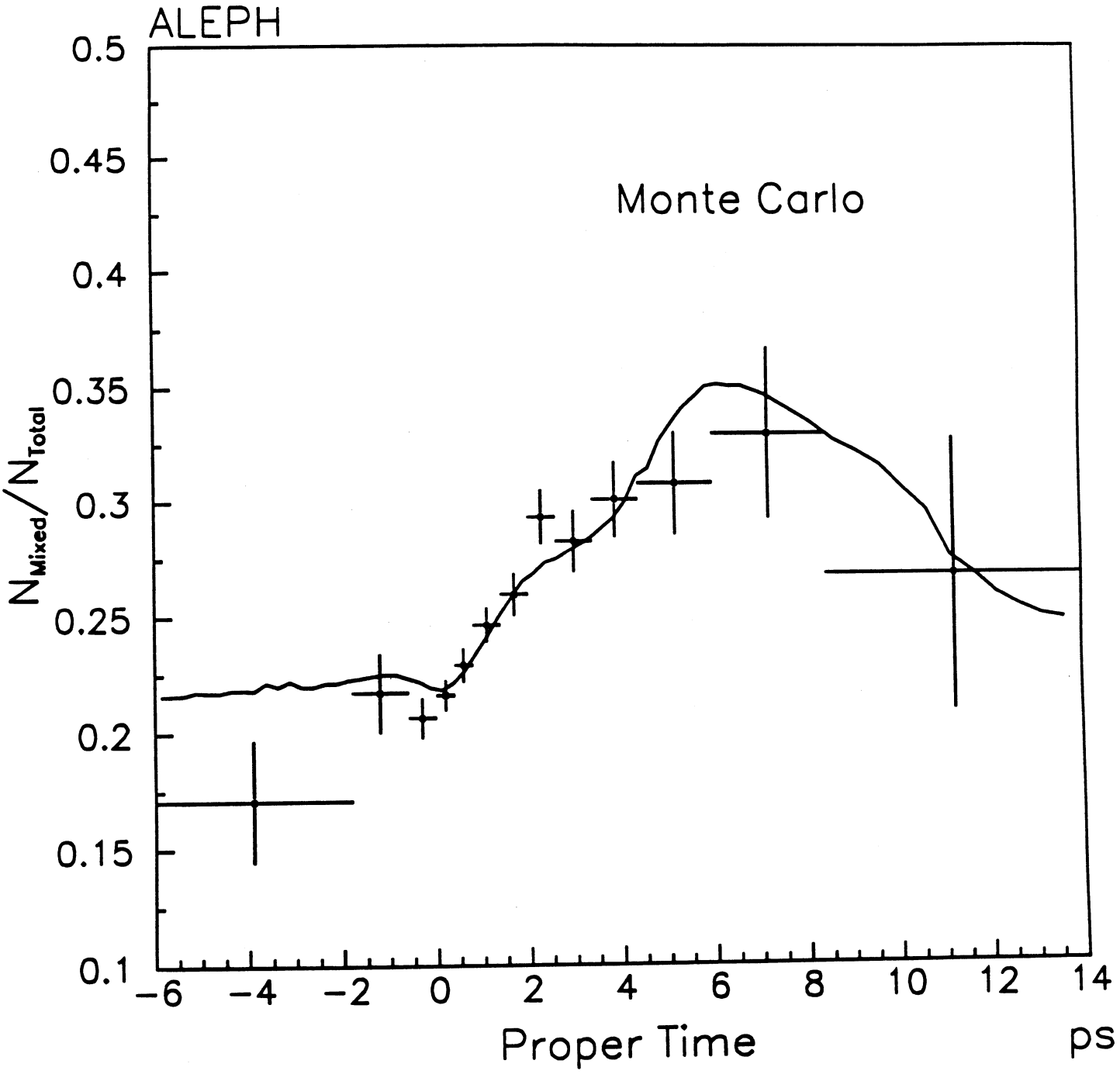

Figure 10(a). The tagged mixed fraction of Monte Carlo events as a function of measured proper time ($\Delta m_s = 1.67\ ps^{-1}$). The expected distribution for $\Delta m_s = 1.67\ ps^{-1}$ is superimposed.

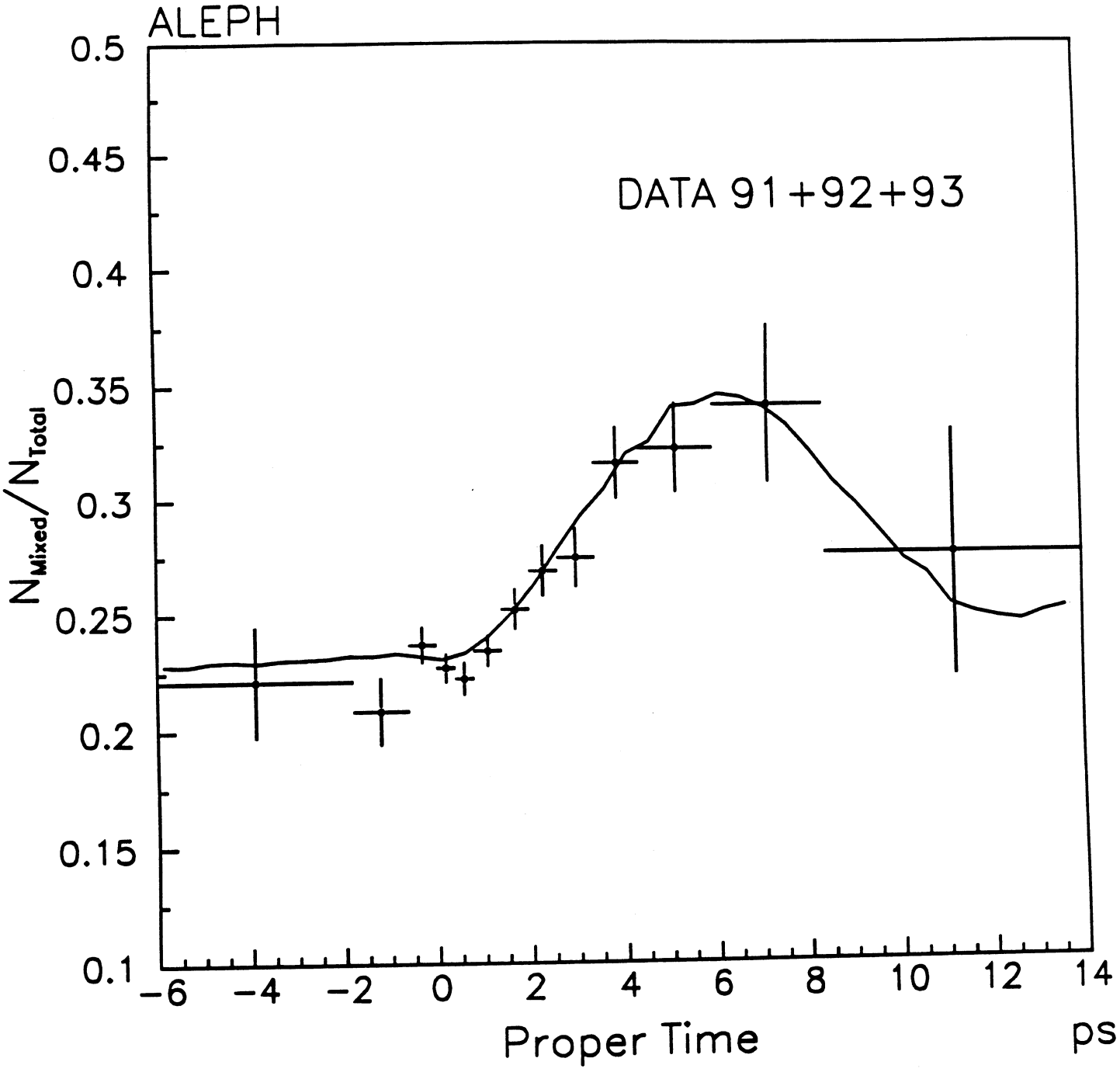

Figure 10(b). The tagged mixed fraction of data events as a function of measured proper time. The expected distribution for $\Delta m_s = 20\ ps^{-1}$ is superimposed.

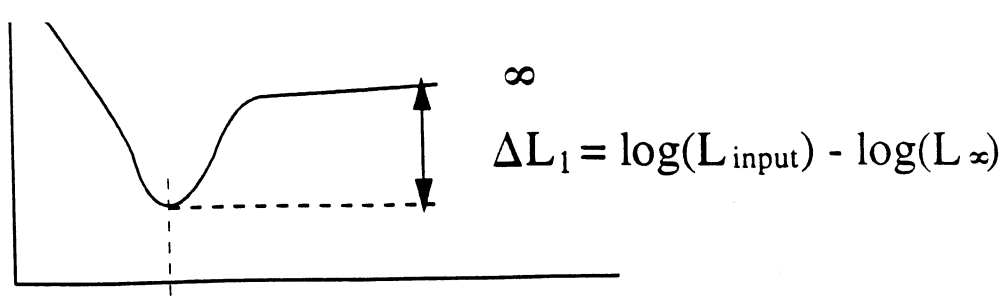

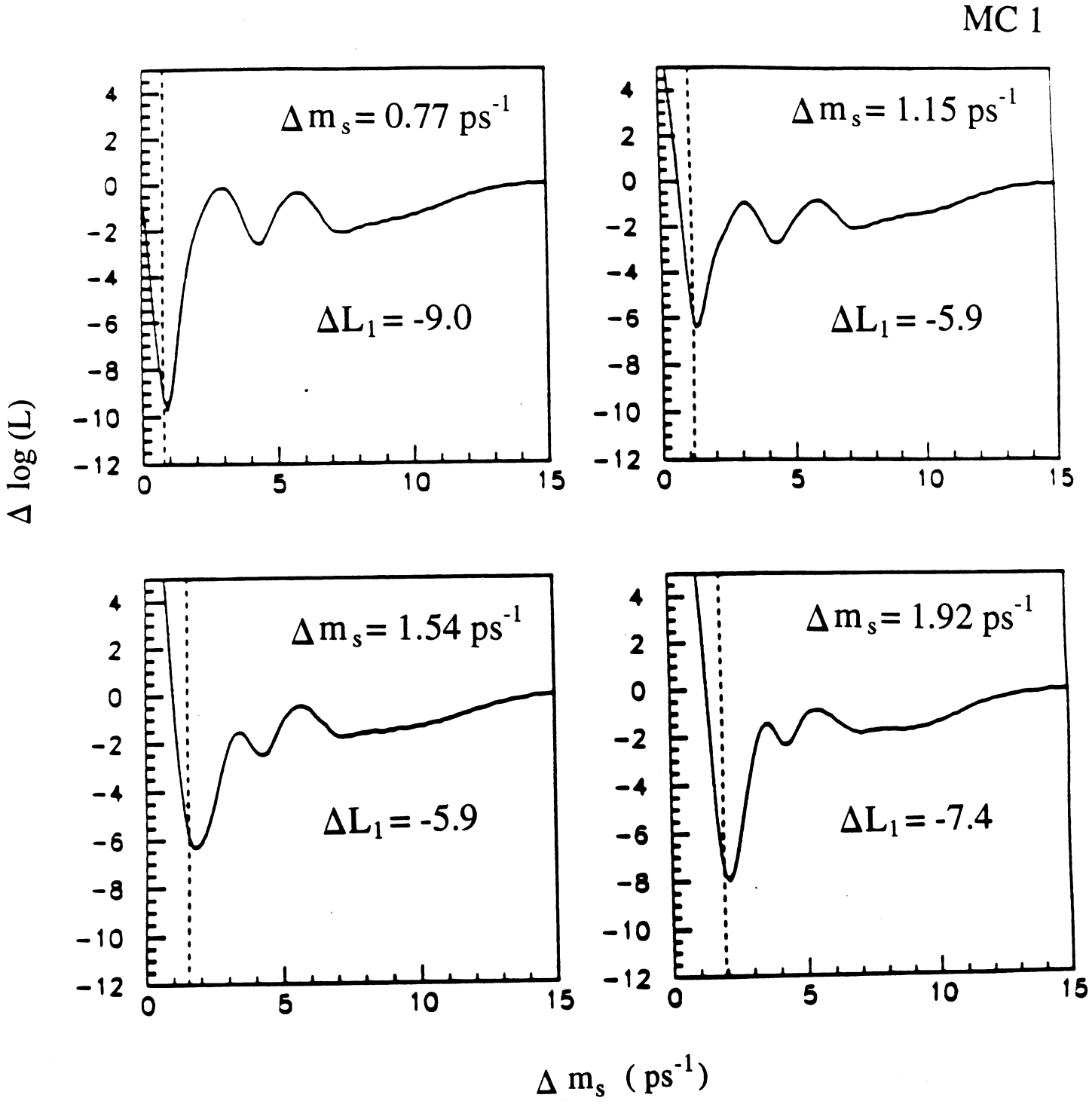

Figure 11(a). *Δln L* scans: *MC 1* (τ_b = *1.3 ps*).

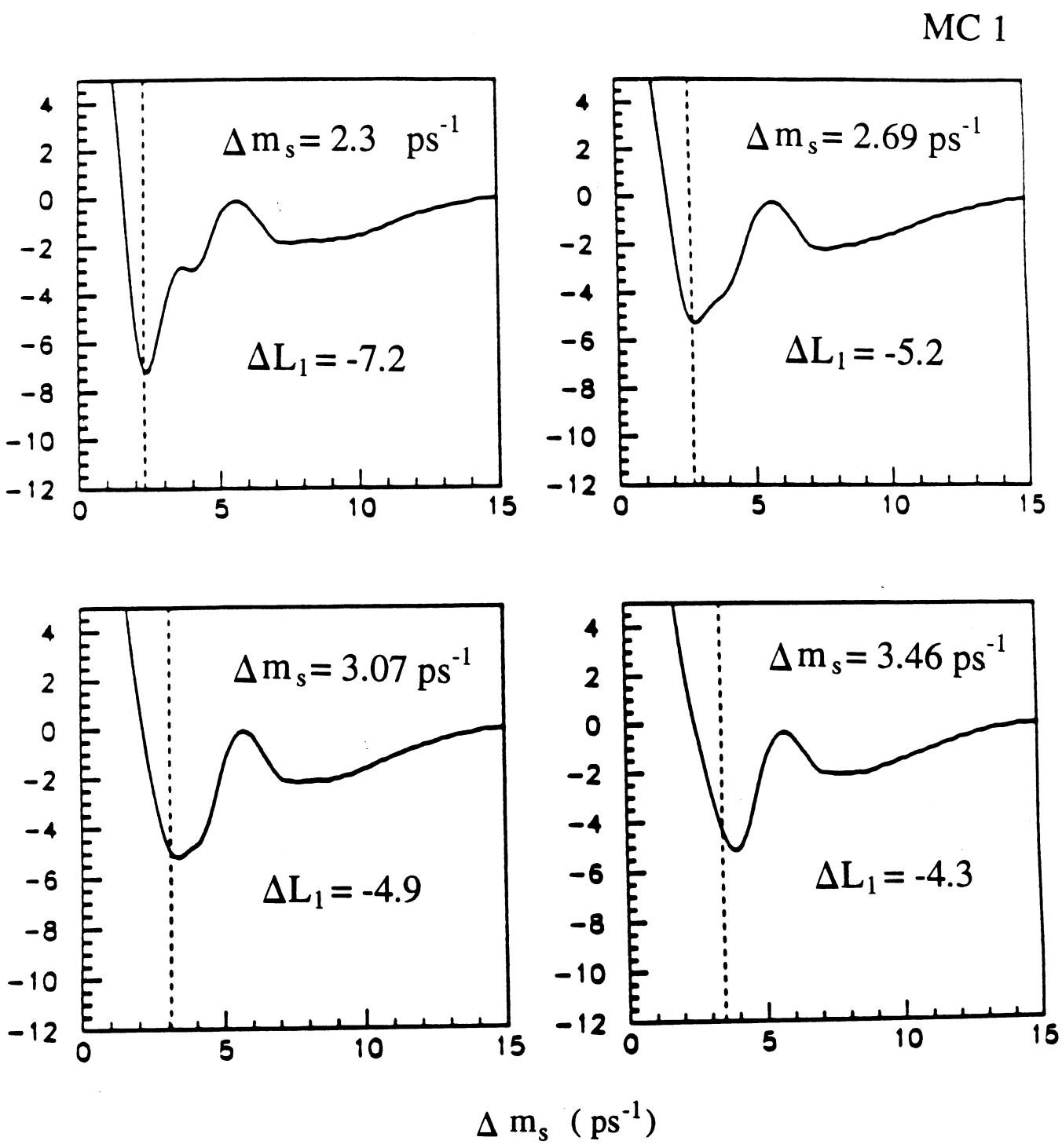

Figure 11(b). *Δln L* scans: *MC 1* ($\tau_b = 1.3$ *ps*).

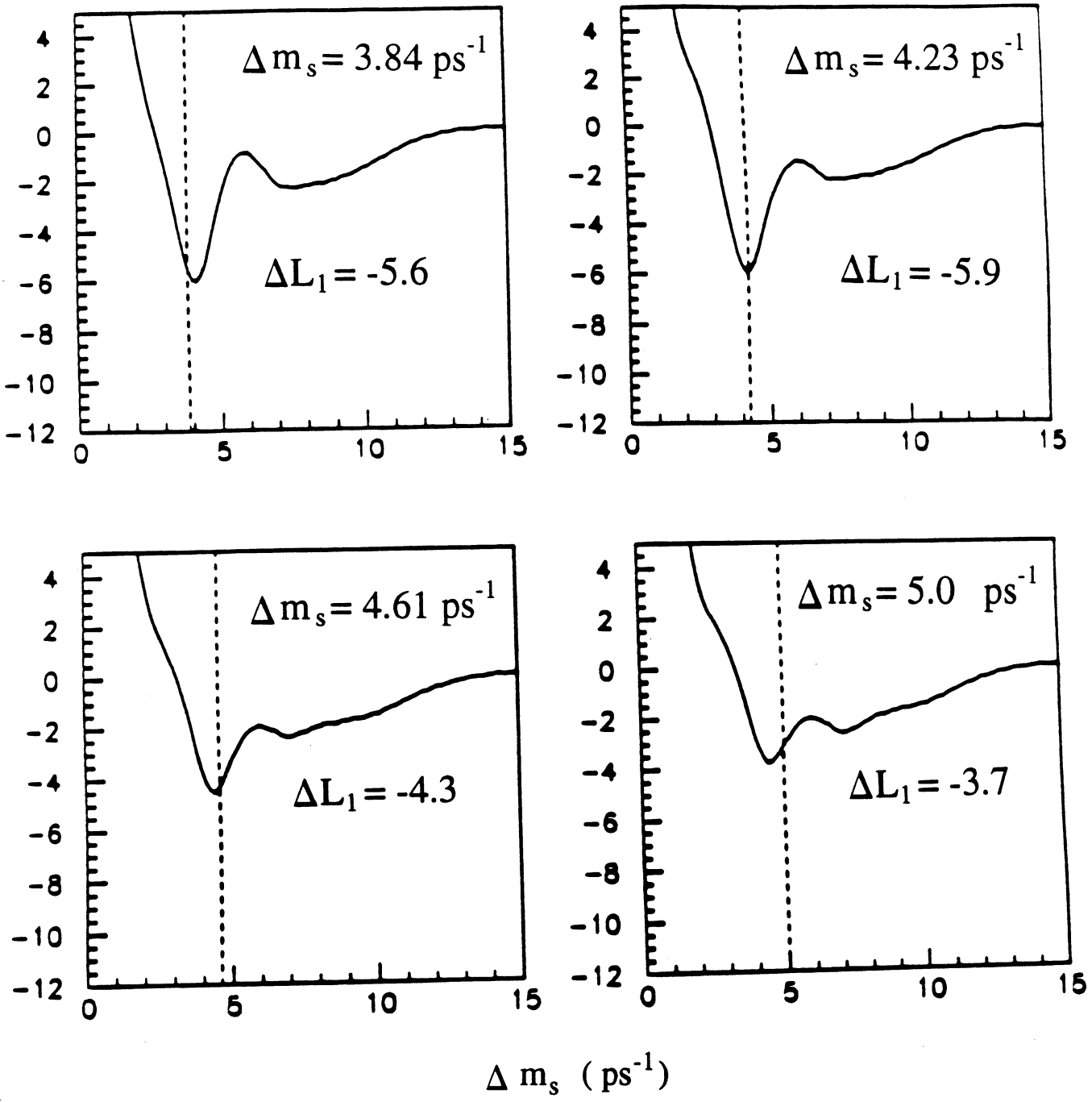

Figure 11(c). *Δln L* scans: *MC 1* (τ_b = *1.3 ps*).

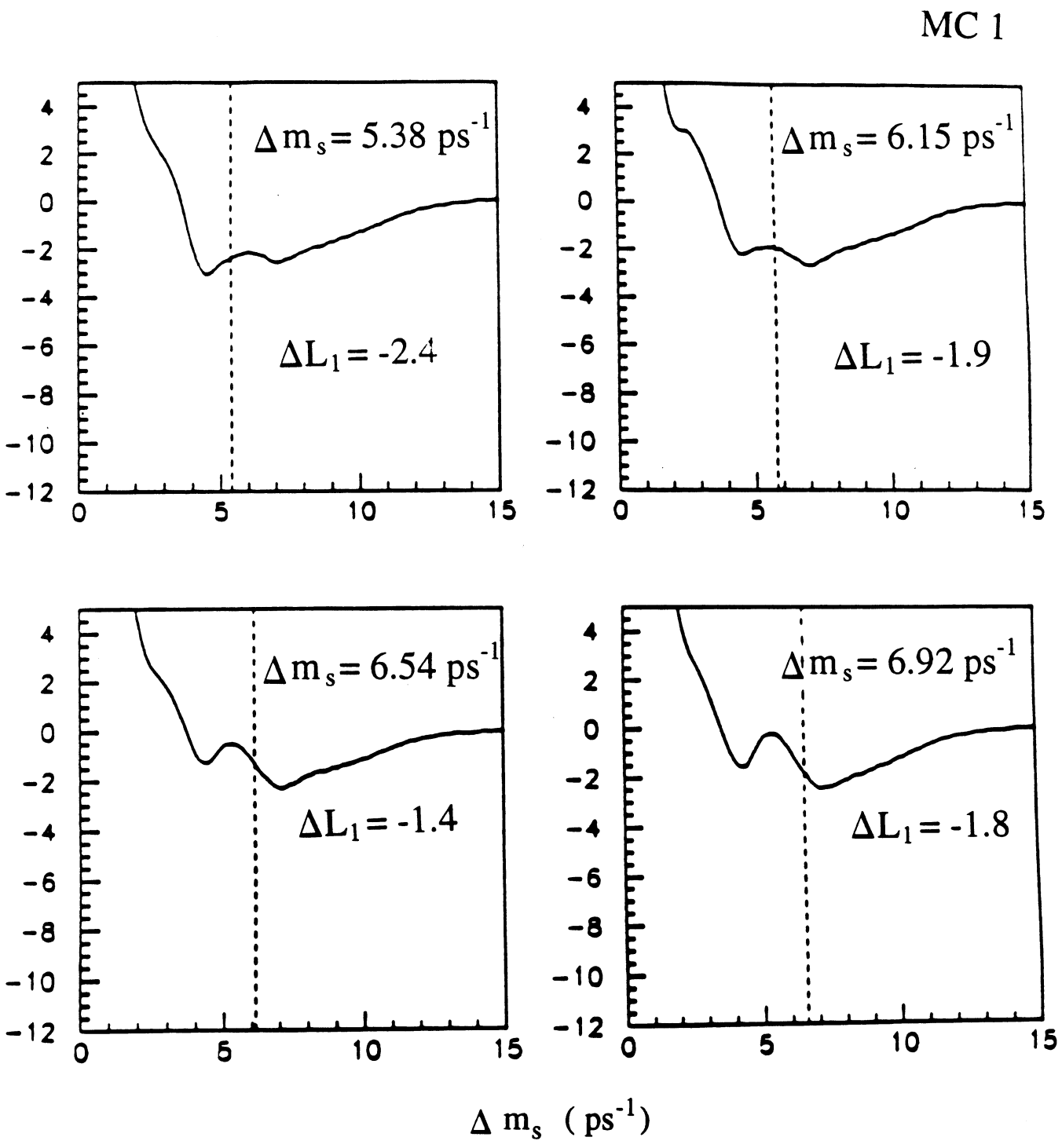

Figure 11(d). *Δln L* scans: *MC 1* (τ_b = *1.3 ps*).

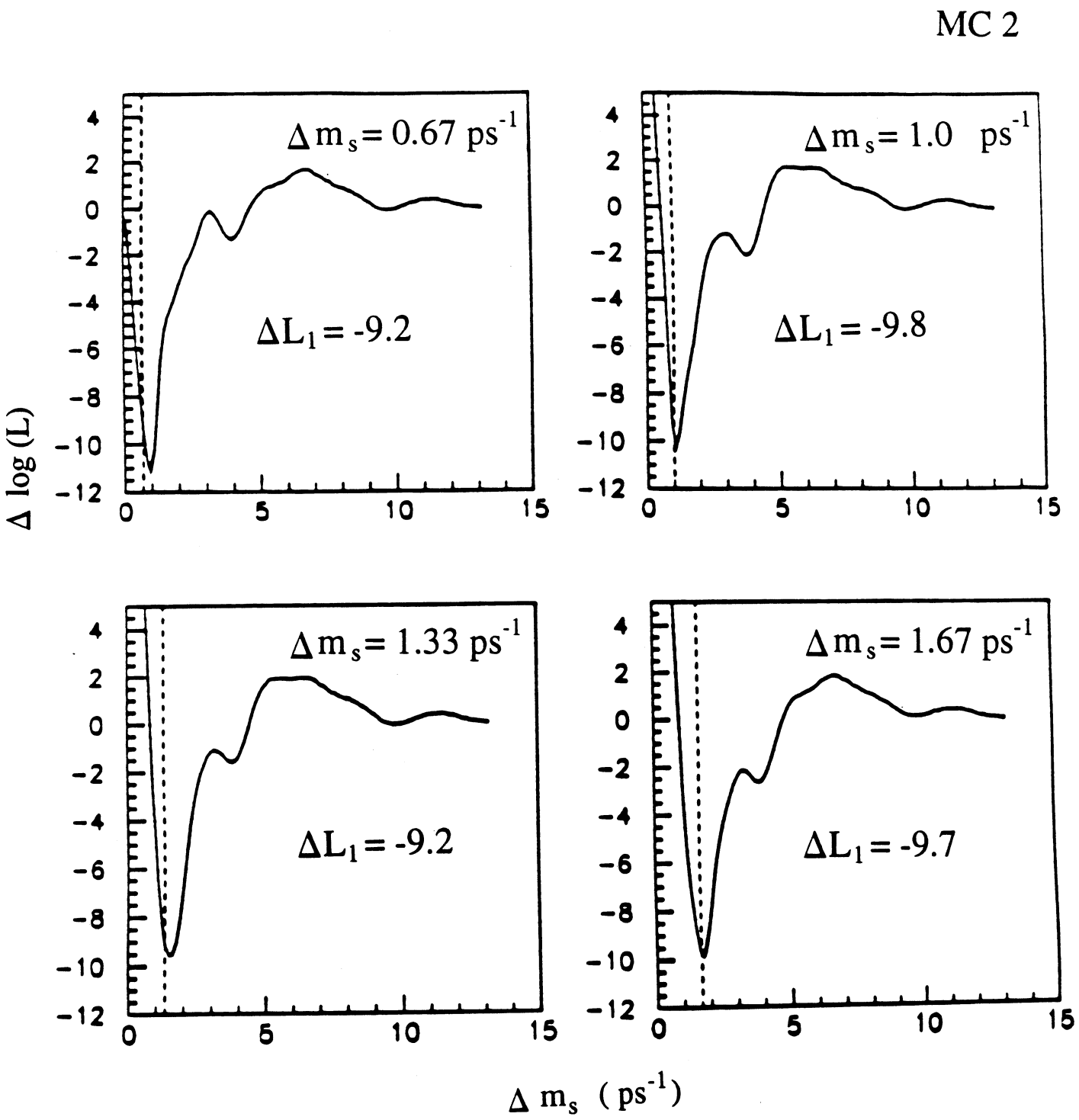

Figure 12(a). *Δln L* scans: *MC 2* (τ_b = *1.5 ps*).

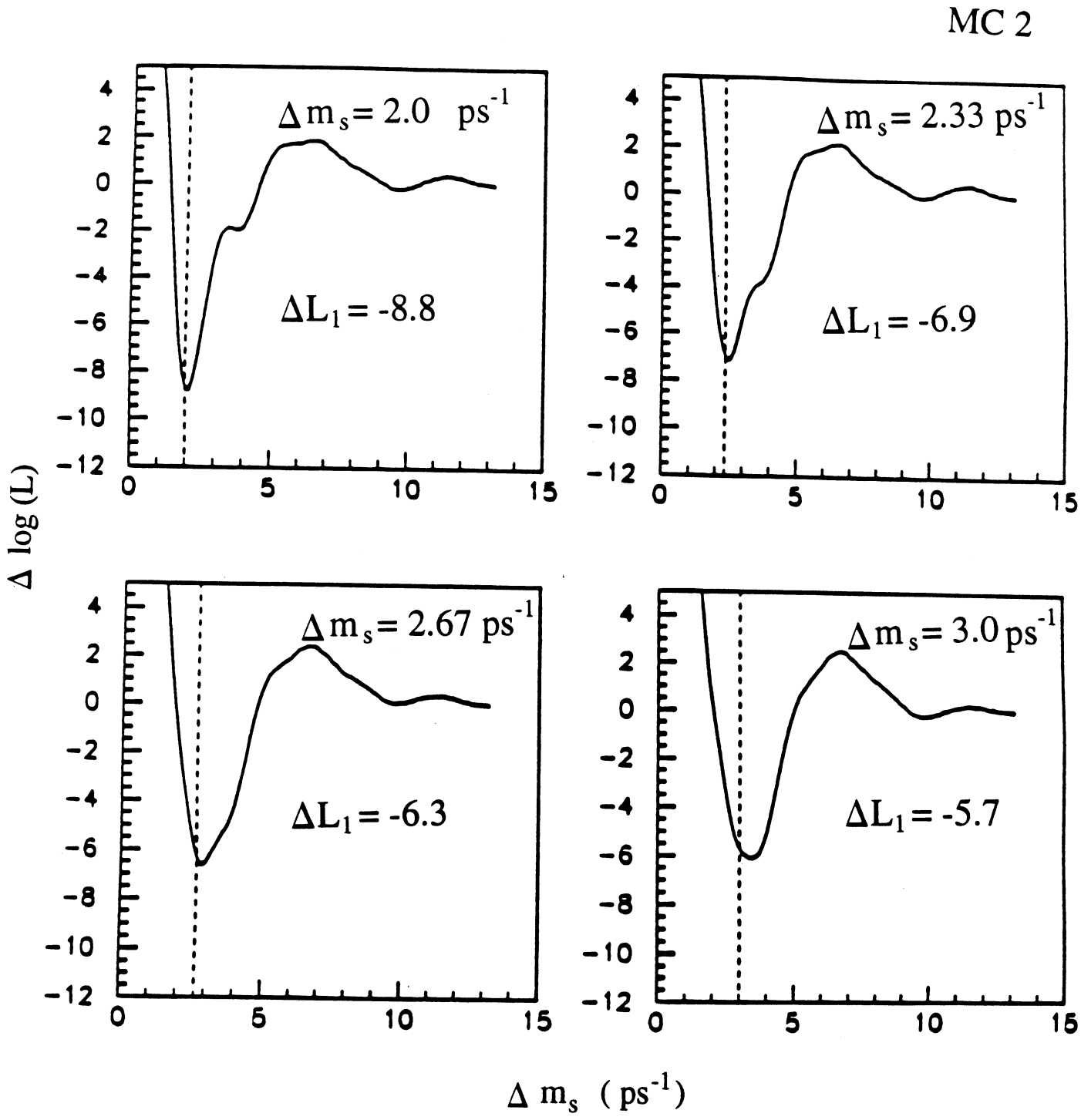

Figure 12(b). *Δln L* scans: *MC 2* ($\tau_b = 1.5ps$).

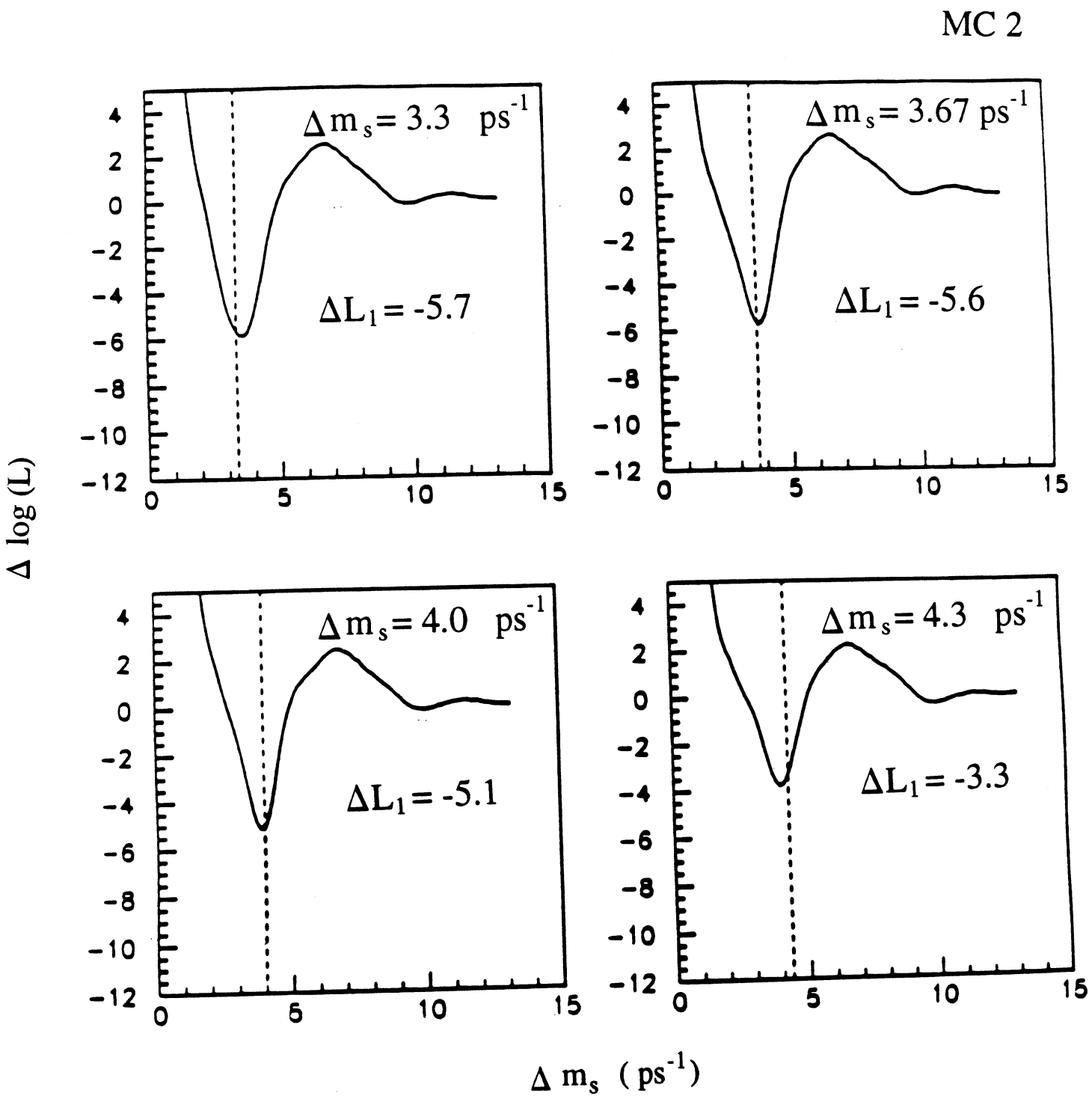

Figure 12(c). $\Delta ln\ L$ scans: *MC 2* ($\tau_b = 1.5 ps$).

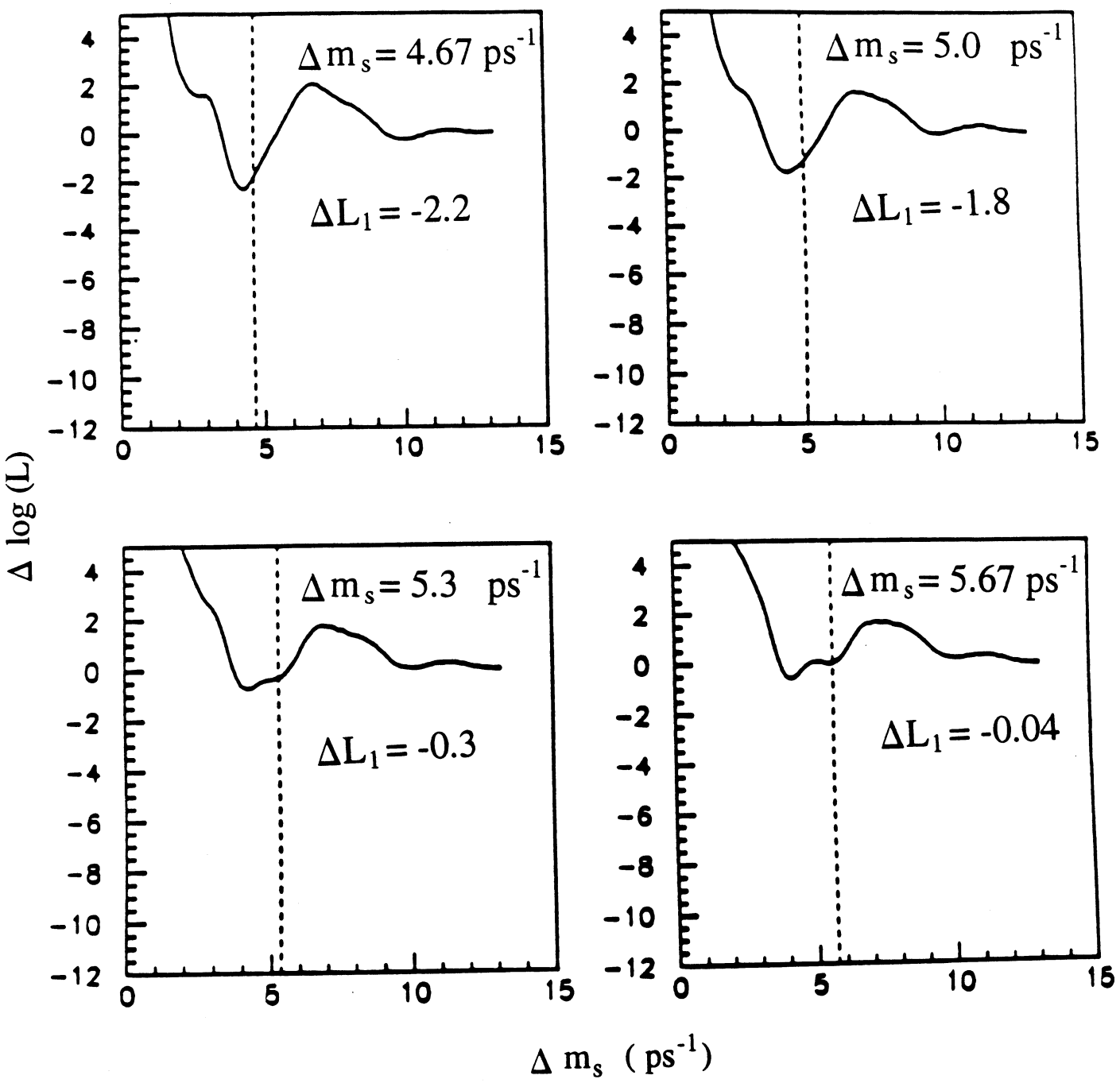

Figure 12(d). *Δln L* scans: *MC 2* ($\tau_b = 1.5ps$).

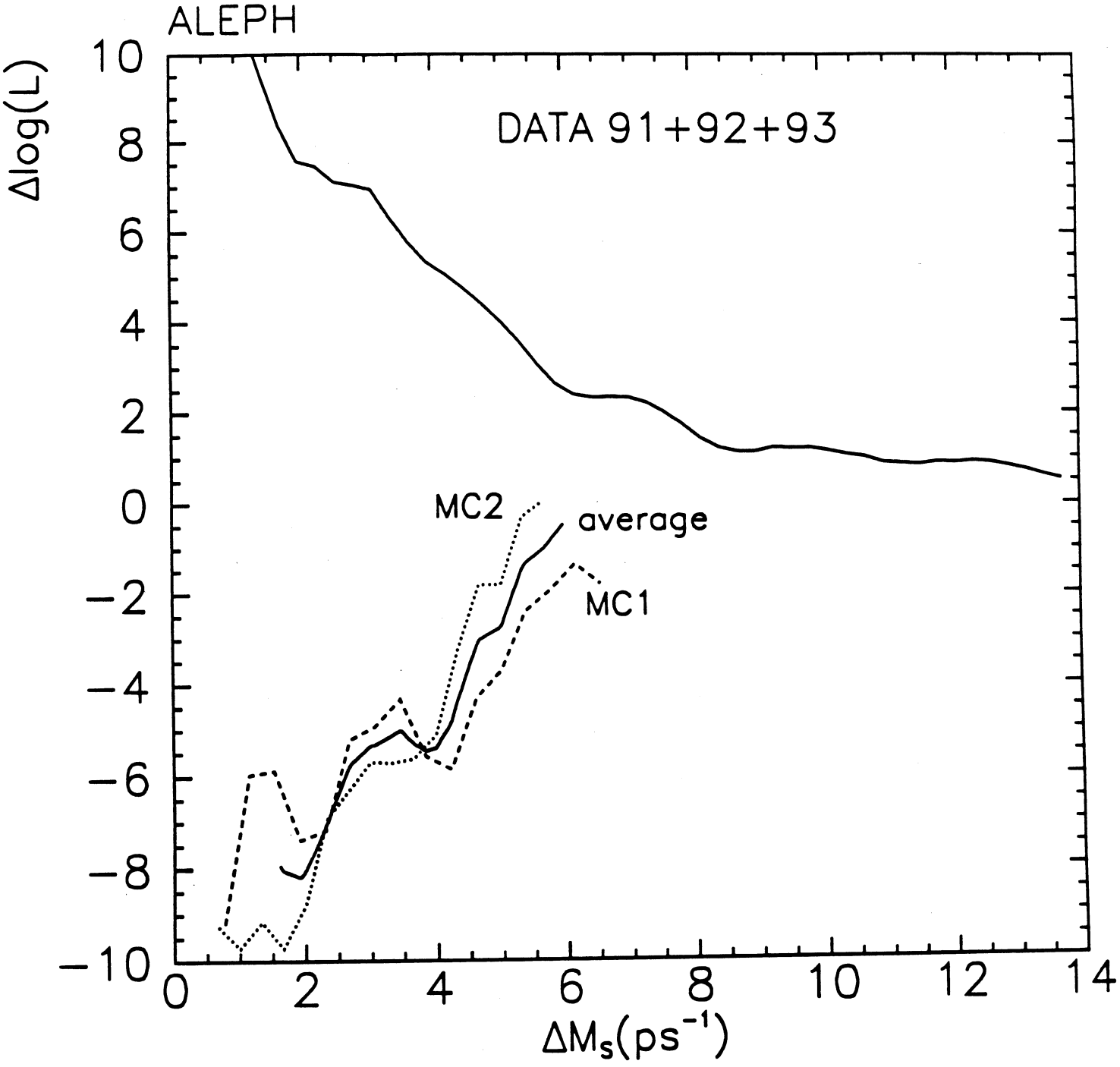

Figure 13. The data $\Delta ln\ L$ curve for the data. Also plotted are the *MC 1* and *MC 2* curves where $\Delta ln\ L$ is measured at the input Δm_s, and their average.

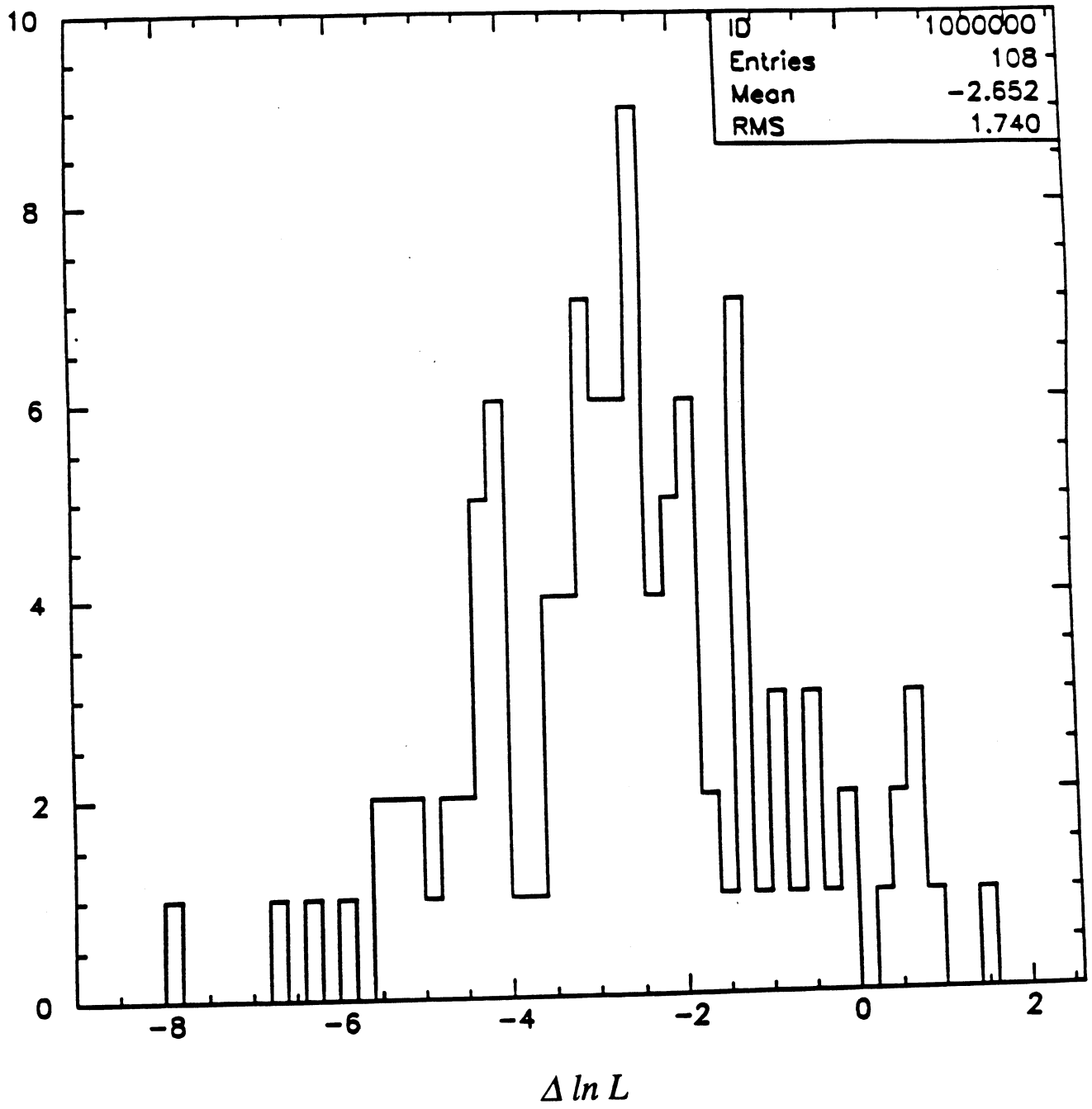

Figure 14(a). The $\Delta ln\ L$ distribution for input $\Delta m_s = 5\ ps^{-1}$.

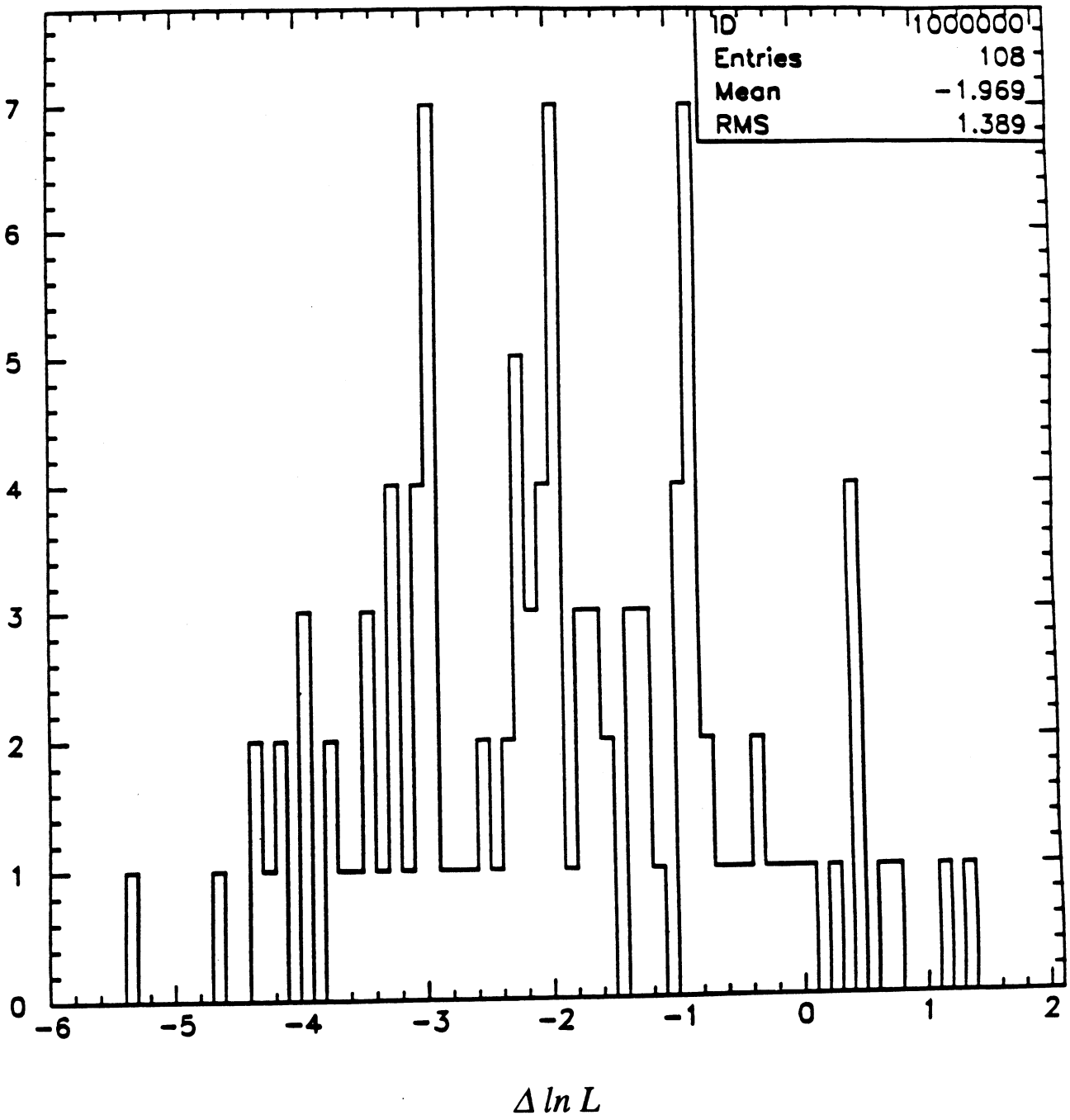

Figure 14(b). The $\Delta ln\, L$ distribution for input $\Delta m_s = 6\ ps^{-1}$.

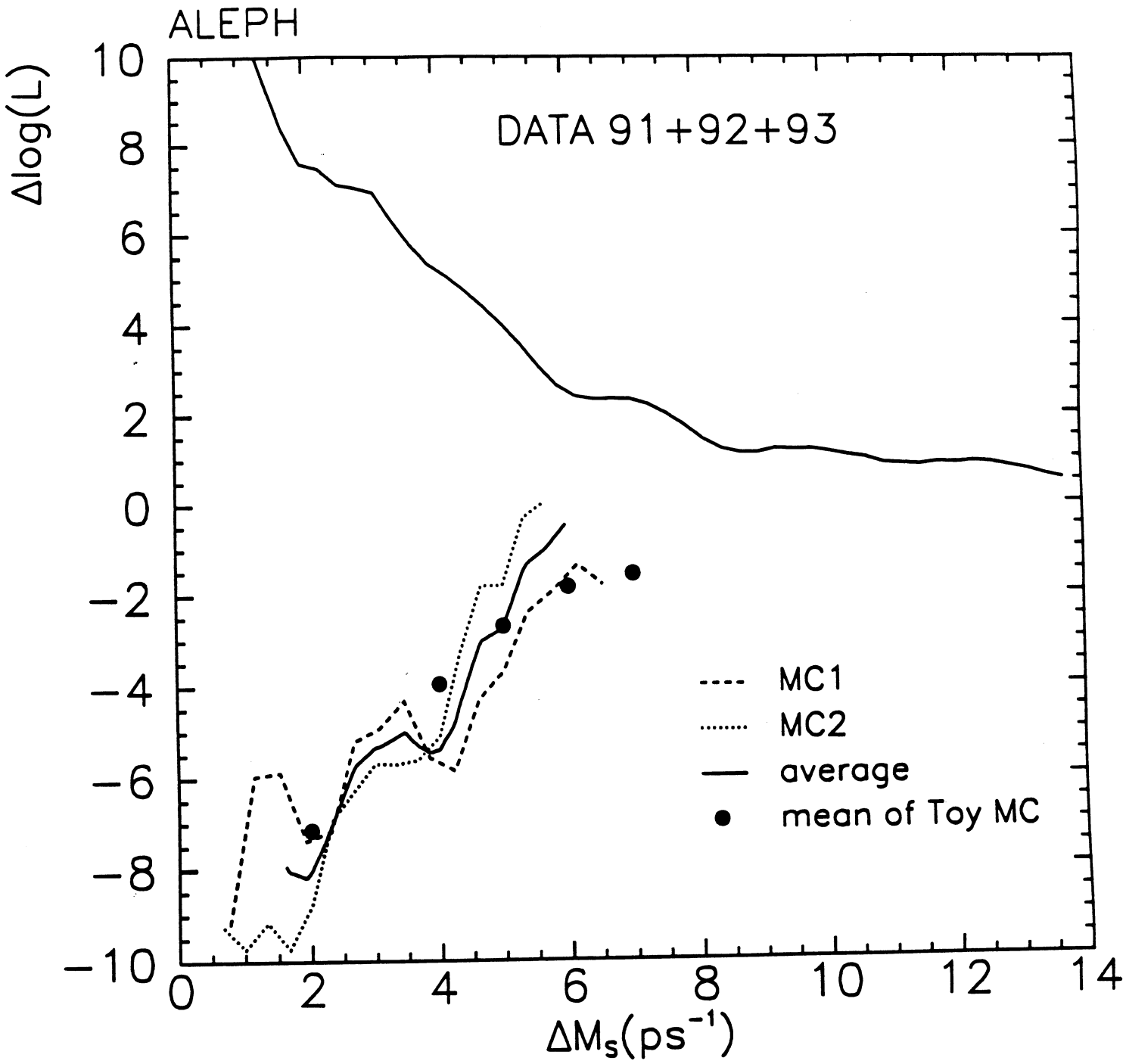

Figure 15. The same *MC 1* and *MC 2* likelihood curves (and their average) as in Fig 13. Superimposed are the average $\Delta ln\ L$ values for various inputs of Δm_s in the toy Monte Carlo.

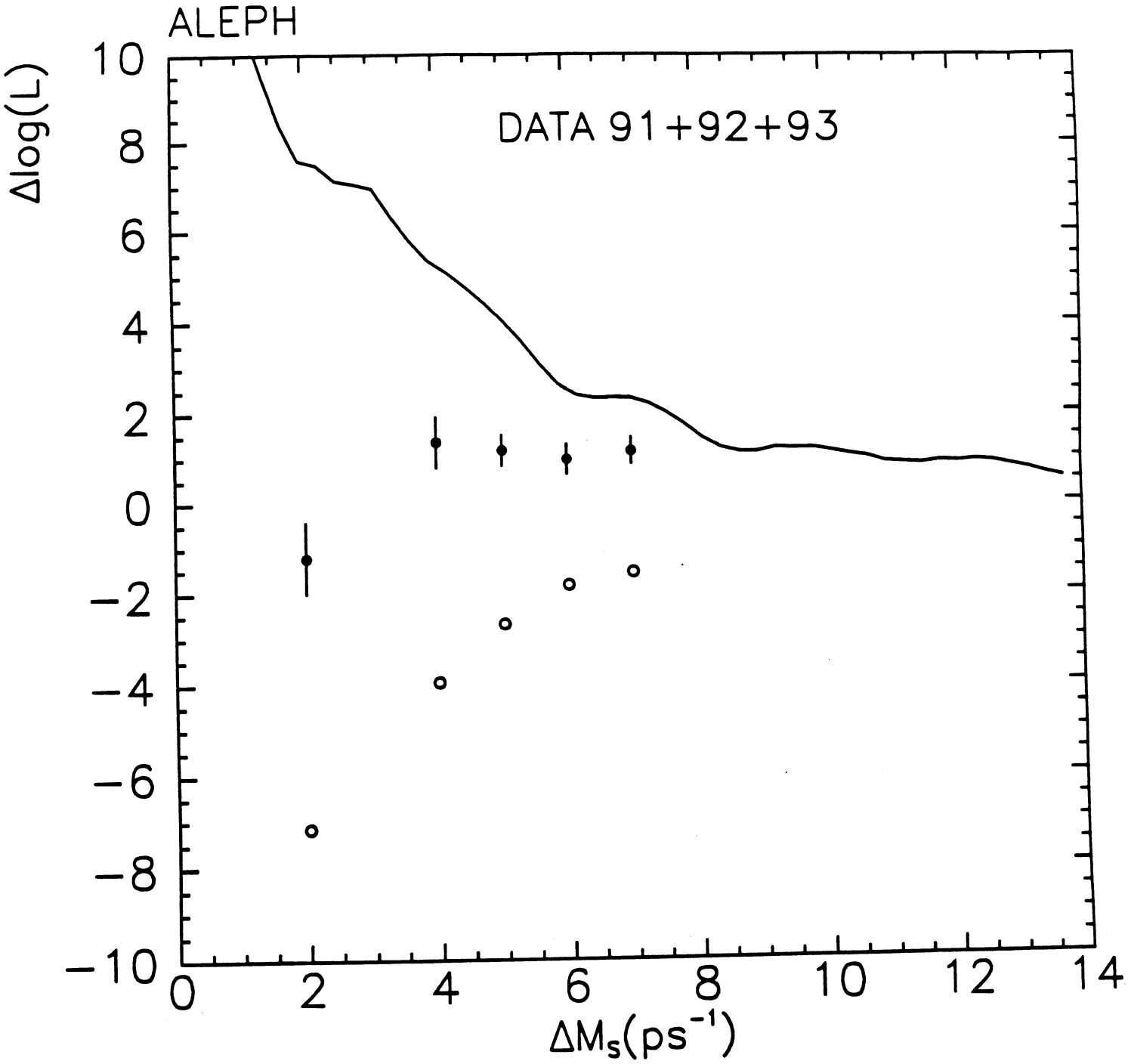

Figure 16(a). Superimposed on the data likelihood curve are the average of the toy Monte Carlo $\Delta ln\ L$ values and the 95% confidence points by counting.

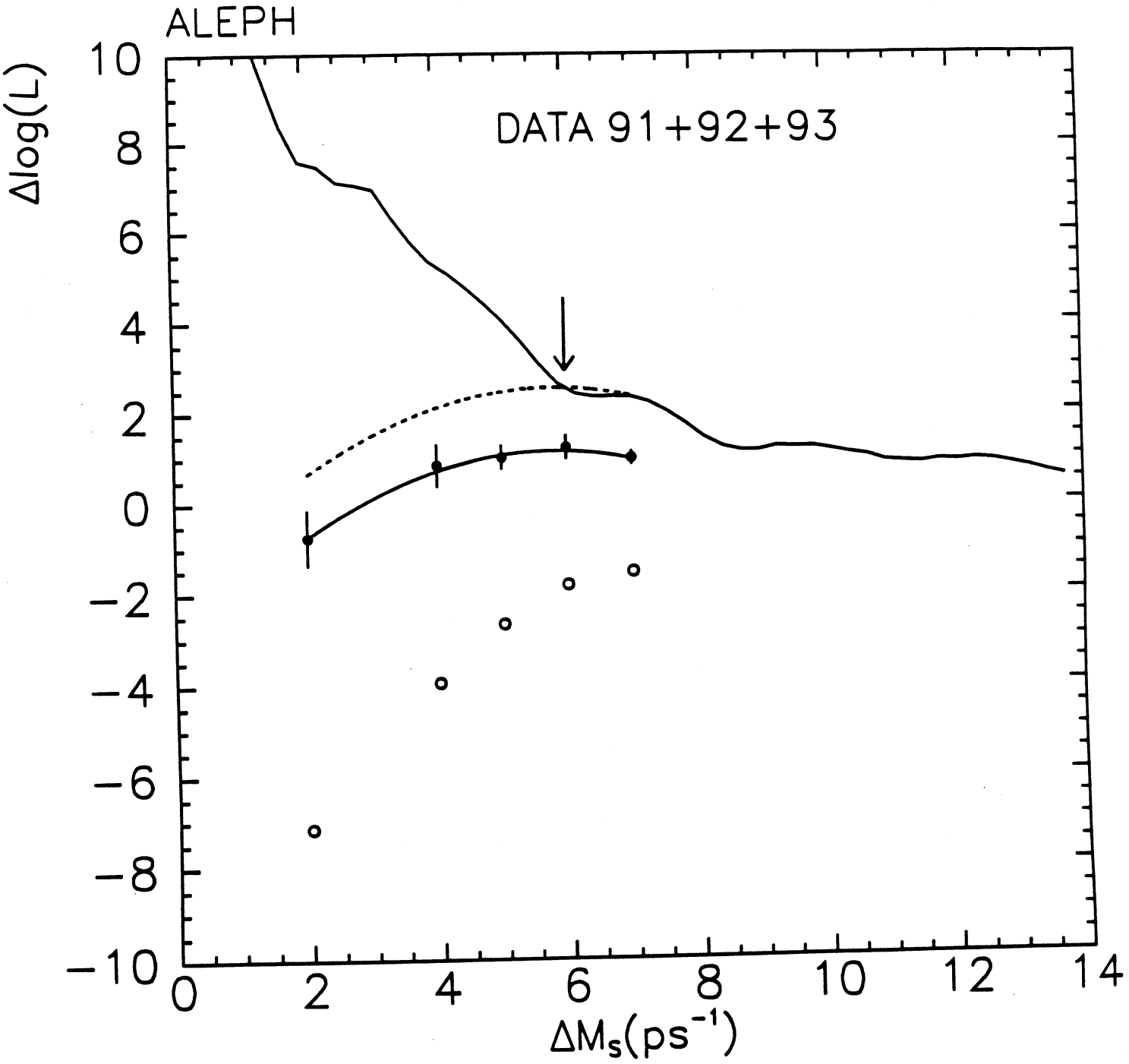

Figure 16(b). Superimposed on the data likelihood curve are the average of the toy Monte Carlo $\Delta ln\ L$ values and the *95%* confidence points by fitting. A *95%* limit curve is fit to the points, and a more conservative limit curve is then raised by *1.4* units.